EUROPEAN LABORATORY FOR PARTICLE PHYSICS

CERN-PPE/97-123
9 September 1997

Search for Unstable Heavy and Excited Leptons in e^+e^- Collisions at $\sqrt{s} = 170$-172 GeV

The OPAL Collaboration

Abstract

We have searched for unstable neutral and charged heavy leptons, N and $L^{\pm}$, and for excited states of neutral and charged leptons, ν^*, e^*, μ^* and τ^*, in e^+e^- collisions at centre-of-mass energies of 170 and 172 GeV using the OPAL detector at LEP. No evidence for their existence was found. From the analysis of charged-current decays of pair-produced unstable heavy leptons, and of charged-current and photonic decays of pair-produced excited leptons, lower limits on their masses are derived. From the analysis of charged-current and photonic decays of singly-produced excited leptons, upper limits on the ratio of the coupling to the compositeness scale, f/Λ, are determined for masses up to the kinematic limit.

Submitted to Z. Phys. C

The OPAL Collaboration

K. Ackerstaff[8], G. Alexander[23], J. Allison[16], N. Altekamp[5], K.J. Anderson[9], S. Anderson[12], S. Arcelli[2], S. Asai[24], D. Axen[29], G. Azuelos[18,a], A.H. Ball[17], E. Barberio[8], R.J. Barlow[16], R. Bartoldus[3], J.R. Batley[5], S. Baumann[3], J. Bechtluft[14], C. Beeston[16], T. Behnke[8], A.N. Bell[1], K.W. Bell[20], G. Bella[23], S. Bentvelsen[8], S. Bethke[14], O. Biebel[14], A. Biguzzi[5], S.D. Bird[16], V. Blobel[27], I.J. Bloodworth[1], J.E. Bloomer[1], M. Bobinski[10], P. Bock[11], D. Bonacorsi[2], M. Boutemeur[34], B.T. Bouwens[12], S. Braibant[12], L. Brigliadori[2], R.M. Brown[20], H.J. Burckhart[8], C. Burgard[8], R. Bürgin[10], P. Capiluppi[2], R.K. Carnegie[6], A.A. Carter[13], J.R. Carter[5], C.Y. Chang[17], D.G. Charlton[1,b], D. Chrisman[4], P.E.L. Clarke[15], I. Cohen[23], J.E. Conboy[15], O.C. Cooke[8], M. Cuffiani[2], S. Dado[22], C. Dallapiccola[17], G.M. Dallavalle[2], R. Davis[30], S. De Jong[12], L.A. del Pozo[4], K. Desch[3], B. Dienes[33,d], M.S. Dixit[7], E. do Couto e Silva[12], M. Doucet[18], E. Duchovni[26], G. Duckeck[34], I.P. Duerdoth[16], D. Eatough[16], J.E.G. Edwards[16], P.G. Estabrooks[6], H.G. Evans[9], M. Evans[13], F. Fabbri[2], M. Fanti[2], A.A. Faust[30], F. Fiedler[27], M. Fierro[2], H.M. Fischer[3], I. Fleck[8], R. Folman[26], D.G. Fong[17], M. Foucher[17], A. Fürtjes[8], D.I. Futyan[16], P. Gagnon[7], J.W. Gary[4], J. Gascon[18], S.M. Gascon-Shotkin[17], N.I. Geddes[20], C. Geich-Gimbel[3], T. Geralis[20], G. Giacomelli[2], P. Giacomelli[4], R. Giacomelli[2], V. Gibson[5], W.R. Gibson[13], D.M. Gingrich[30,a], D. Glenzinski[9], J. Goldberg[22], M.J. Goodrick[5], W. Gorn[4], C. Grandi[2], E. Gross[26], J. Grunhaus[23], M. Gruwé[8], C. Hajdu[32], G.G. Hanson[12], M. Hansroul[8], M. Hapke[13], C.K. Hargrove[7], P.A. Hart[9], C. Hartmann[3], M. Hauschild[8], C.M. Hawkes[5], R. Hawkings[27], R.J. Hemingway[6], M. Herndon[17], G. Herten[10], R.D. Heuer[8], M.D. Hildreth[8], J.C. Hill[5], S.J. Hillier[1], P.R. Hobson[25], R.J. Homer[1], A.K. Honma[28,a], D. Horváth[32,c], K.R. Hossain[30], R. Howard[29], P. Hüntemeyer[27], D.E. Hutchcroft[5], P. Igo-Kemenes[11], D.C. Imrie[25], M.R. Ingram[16], K. Ishii[24], A. Jawahery[17], P.W. Jeffreys[20], H. Jeremie[18], M. Jimack[1], A. Joly[18], C.R. Jones[5], G. Jones[16], M. Jones[6], U. Jost[11], P. Jovanovic[1], T.R. Junk[8], D. Karlen[6], V. Kartvelishvili[16], K. Kawagoe[24], T. Kawamoto[24], P.I. Kayal[30], R.K. Keeler[28], R.G. Kellogg[17], B.W. Kennedy[20], J. Kirk[29], A. Klier[26], S. Kluth[8], T. Kobayashi[24], M. Kobel[10], D.S. Koetke[6], T.P. Kokott[3], M. Kolrep[10], S. Komamiya[24], T. Kress[11], P. Krieger[6], J. von Krogh[11], P. Kyberd[13], G.D. Lafferty[16], R. Lahmann[17], W.P. Lai[19], D. Lanske[14], J. Lauber[15], S.R. Lautenschlager[31], J.G. Layter[4], D. Lazic[22], A.M. Lee[31], E. Lefebvre[18], D. Lellouch[26], J. Letts[12], L. Levinson[26], S.L. Lloyd[13], F.K. Loebinger[16], G.D. Long[28], M.J. Losty[7], J. Ludwig[10], A. Macchiolo[2], A. Macpherson[30], M. Mannelli[8], S. Marcellini[2], C. Markus[3], A.J. Martin[13], J.P. Martin[18], G. Martinez[17], T. Mashimo[24], P. Mättig[3], W.J. McDonald[30], J. McKenna[29], E.A. Mckigney[15], T.J. McMahon[1], R.A. McPherson[8], F. Meijers[8], S. Menke[3], F.S. Merritt[9], H. Mes[7], J. Meyer[27], A. Michelini[2], G. Mikenberg[26], D.J. Miller[15], A. Mincer[22,e], R. Mir[26], W. Mohr[10], A. Montanari[2], T. Mori[24], M. Morii[24], U. Müller[3], S. Mihara[24], K. Nagai[26], I. Nakamura[24], H.A. Neal[8], B. Nellen[3], R. Nisius[8], S.W. O'Neale[1], F.G. Oakham[7], F. Odorici[2], H.O. Ogren[12], A. Oh[27], N.J. Oldershaw[16], M.J. Oreglia[9], S. Orito[24], J. Pálinkás[33,d], G. Pásztor[32], J.R. Pater[16], G.N. Patrick[20], J. Patt[10], M.J. Pearce[1], R. Perez-Ochoa[8], S. Petzold[27], P. Pfeifenschneider[14], J.E. Pilcher[9], J. Pinfold[30], D.E. Plane[8], P. Poffenberger[28], B. Poli[2], A. Posthaus[3], D.L. Rees[1], D. Rigby[1], S. Robertson[28], S.A. Robins[22], N. Rodning[30], J.M. Roney[28], A. Rooke[15], E. Ros[8], A.M. Rossi[2], P. Routenburg[30], Y. Rozen[22], K. Runge[10], O. Runolfsson[8], U. Ruppel[14], D.R. Rust[12], R. Rylko[25], K. Sachs[10], T. Saeki[24], E.K.G. Sarkisyan[23], C. Sbarra[29], A.D. Schaile[34], O. Schaile[34], F. Scharf[3], P. Scharff-Hansen[8], P. Schenk[34], J. Schieck[11], P. Schleper[11], B. Schmitt[8], S. Schmitt[11], A. Schöning[8], M. Schröder[8], H.C. Schultz-Coulon[10], M. Schumacher[3], C. Schwick[8], W.G. Scott[20], T.G. Shears[16], B.C. Shen[4], C.H. Shepherd-Themistocleous[8],

P. Sherwood[15], G.P. Siroli[2], A. Sittler[27], A. Skillman[15], A. Skuja[17], A.M. Smith[8], G.A. Snow[17], R. Sobie[28], S. Söldner-Rembold[10], R.W. Springer[30], M. Sproston[20], K. Stephens[16], J. Steuerer[27], B. Stockhausen[3], K. Stoll[10], D. Strom[19], P. Szymanski[20], R. Tafirout[18], S.D. Talbot[1], S. Tanaka[24], P. Taras[18], S. Tarem[22], R. Teuscher[8], M. Thiergen[10], M.A. Thomson[8], E. von Törne[3], S. Towers[6], I. Trigger[18], Z. Trócsányi[33], E. Tsur[23], A.S. Turcot[9], M.F. Turner-Watson[8], P. Utzat[11], R. Van Kooten[12], M. Verzocchi[10], P. Vikas[18], E.H. Vokurka[16], H. Voss[3], F. Wäckerle[10], A. Wagner[27], C.P. Ward[5], D.R. Ward[5], P.M. Watkins[1], A.T. Watson[1], N.K. Watson[1], P.S. Wells[8], N. Wermes[3], J.S. White[28], B. Wilkens[10], G.W. Wilson[27], J.A. Wilson[1], G. Wolf[26], T.R. Wyatt[16], S. Yamashita[24], G. Yekutieli[26], V. Zacek[18], D. Zer-Zion[8]

[1]School of Physics and Space Research, University of Birmingham, Birmingham B15 2TT, UK
[2]Dipartimento di Fisica dell' Università di Bologna and INFN, I-40126 Bologna, Italy
[3]Physikalisches Institut, Universität Bonn, D-53115 Bonn, Germany
[4]Department of Physics, University of California, Riverside CA 92521, USA
[5]Cavendish Laboratory, Cambridge CB3 0HE, UK
[6] Ottawa-Carleton Institute for Physics, Department of Physics, Carleton University, Ottawa, Ontario K1S 5B6, Canada
[7]Centre for Research in Particle Physics, Carleton University, Ottawa, Ontario K1S 5B6, Canada
[8]CERN, European Organisation for Particle Physics, CH-1211 Geneva 23, Switzerland
[9]Enrico Fermi Institute and Department of Physics, University of Chicago, Chicago IL 60637, USA
[10]Fakultät für Physik, Albert Ludwigs Universität, D-79104 Freiburg, Germany
[11]Physikalisches Institut, Universität Heidelberg, D-69120 Heidelberg, Germany
[12]Indiana University, Department of Physics, Swain Hall West 117, Bloomington IN 47405, USA
[13]Queen Mary and Westfield College, University of London, London E1 4NS, UK
[14]Technische Hochschule Aachen, III Physikalisches Institut, Sommerfeldstrasse 26-28, D-52056 Aachen, Germany
[15]University College London, London WC1E 6BT, UK
[16]Department of Physics, Schuster Laboratory, The University, Manchester M13 9PL, UK
[17]Department of Physics, University of Maryland, College Park, MD 20742, USA
[18]Laboratoire de Physique Nucléaire, Université de Montréal, Montréal, Quebec H3C 3J7, Canada
[19]University of Oregon, Department of Physics, Eugene OR 97403, USA
[20]Rutherford Appleton Laboratory, Chilton, Didcot, Oxfordshire OX11 0QX, UK
[22]Department of Physics, Technion-Israel Institute of Technology, Haifa 32000, Israel
[23]Department of Physics and Astronomy, Tel Aviv University, Tel Aviv 69978, Israel
[24]International Centre for Elementary Particle Physics and Department of Physics, University of Tokyo, Tokyo 113, and Kobe University, Kobe 657, Japan
[25]Brunel University, Uxbridge, Middlesex UB8 3PH, UK
[26]Particle Physics Department, Weizmann Institute of Science, Rehovot 76100, Israel
[27]Universität Hamburg/DESY, II Institut für Experimental Physik, Notkestrasse 85, D-22607 Hamburg, Germany
[28]University of Victoria, Department of Physics, P O Box 3055, Victoria BC V8W 3P6, Canada
[29]University of British Columbia, Department of Physics, Vancouver BC V6T 1Z1, Canada

[30]University of Alberta, Department of Physics, Edmonton AB T6G 2J1, Canada
[31]Duke University, Dept of Physics, Durham, NC 27708-0305, USA
[32]Research Institute for Particle and Nuclear Physics, H-1525 Budapest, P O Box 49, Hungary
[33]Institute of Nuclear Research, H-4001 Debrecen, P O Box 51, Hungary
[34]Ludwigs-Maximilians-Universität München, Sektion Physik, Am Coulombwall 1, D-85748 Garching, Germany

[a] and at TRIUMF, Vancouver, Canada V6T 2A3
[b] and Royal Society University Research Fellow
[c] and Institute of Nuclear Research, Debrecen, Hungary
[d] and Department of Experimental Physics, Lajos Kossuth University, Debrecen, Hungary
[e] and Department of Physics, New York University, NY 1003, USA

1 Introduction

In spite of its remarkable success in describing all electroweak data available today, the Standard Model leaves many questions unanswered. In particular, it does not explain the number of fermion generations nor the fermion mass spectrum. The precise measurements of the Z-boson parameters in e^+e^- collisions at centre-of-mass energies, $\sqrt{s}$, around the Z-boson mass, M_Z, have determined the number of species of light neutrinos to be three [1]; however, this does not exclude a fourth generation, or other more exotic massive fermions, if all of the new particles have masses greater than $M_Z/2$. New fermions could be of the following types (for a review see Reference [2]): (i) sequential fermions, (ii) mirror fermions (with chirality opposite to those of the Standard Model), (iii) vector fermions (with left- and right-handed doublets) and (iv) singlet fermions. These new fermions could be produced at high energy e^+e^- colliders such as LEP, where two production mechanisms are possible: (i) pair-production, and (ii) single-production in association with a light standard fermion from the three known generations. We concentrate on the search for the pair-production of new unstable heavy leptons and for both pair- and single-production of excited states of the known leptons in e^+e^- collisions at centre-of-mass energies up to $\sqrt{s} = 172.3$ GeV. The results will be interpreted in terms of sequential and excited lepton models.

Lower limits on the masses of heavy leptons were obtained at $\sqrt{s} \sim M_Z$ [1, 3], and recent searches at $\sqrt{s} = 130$–140 GeV [4, 5] and $\sqrt{s} = 161$ GeV [6] have improved these limits. The L3 Collaboration has also reported results on sequential heavy lepton searches up to $\sqrt{s} = 172$ GeV [7]. Excited leptons have been sought at the LEP e^+e^- collider at $\sqrt{s} \sim M_Z$ [8], $\sqrt{s} = 130$-140 GeV [9, 10] and $\sqrt{s} = 161$ GeV [11, 12], and at the HERA ep collider [13]. Processes such as $e^+e^- \to \gamma\gamma$ and $e^+e^- \to f\bar{f}$ are sensitive to new particles at higher mass scales but have less sensitivity than direct searches if direct production is kinematically allowed [14, 15].

1.1 Heavy Leptons

We assume mixing with at most one of the light standard leptonic generations in order to avoid leptonic flavour-changing neutral currents (FCNC) at the one-loop level. General new heavy leptons could in principle decay through the charge-current (CC) or the neutral-current (NC) channels:

$$\begin{aligned} N \to \ell^\pm W^\mp \quad , \quad N \to L^\pm W^\mp \quad , \quad N \to \nu_\ell Z, \\ L^\pm \to \nu_\ell W^\pm \quad , \quad L^\pm \to N W^\pm \quad , \quad L^\pm \to \ell^\pm Z, \end{aligned}$$

where N is a neutral heavy lepton, $L^\pm$ is a charged heavy lepton, and $\ell = e$, μ or τ. For heavy lepton masses less than the boson mass, M_W or M_Z, the vector bosons are virtual, leading to a 3-body decay topology. For masses greater than M_W or M_Z, the decays are 2-body, and the CC and NC branching ratios can be comparable. For masses close to M_W or M_Z, it is important to treat the transition from the 3-body to the 2-body decay properly, including effects from the vector boson widths. Expressions for the computation of partial decay widths with an off-shell W or Z can be found in [16]. A mixing angle (ζ) of the heavy lepton with the standard lepton flavour of 0.01 yields a decay length $c\tau$ of $\mathcal{O}(1$ nm); since the decay length is proportional to $1/\zeta^2$, by looking for unstable heavy leptons with efficiency for decays with radii $\mathcal{O}(1$ cm), we

remain sensitive down to mixing angles squared $\mathcal{O}(10^{-12})$. The present upper limit on ζ^2 is approximately 0.005 [17].

Furthermore, we limit ourselves to the case where N and $L^{\pm}$ decay via the CC channel only, as would be expected in a naive fourth generation extension to the Standard Model. In fact, since the new mass region to which we are most sensitive is near M_W, the CC channel should dominate even for more exotic heavy leptons.

There are several possible new heavy lepton discovery channels, depending on the charge of the lightest new heavy lepton and its decay modes. We conduct three different analyses to ensure coverage of these channels:

(A) $e^+e^- \to N\bar{N}$ with a flavour-mixing decay into a light lepton, $N \to eW$, $N \to \mu W$ or $N \to \tau W$. For a Dirac- and a Majorana- ($N = \bar{N}$) type of neutral heavy lepton:

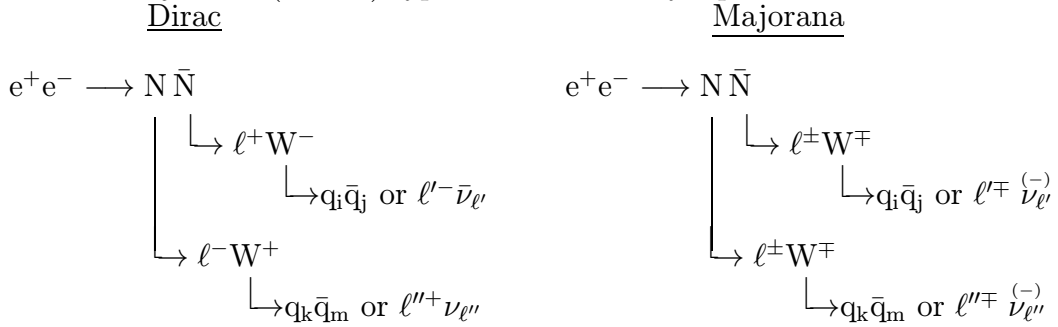

The typical signature of such an event is at least two isolated charged leptons plus the decay products of the two W bosons. In the Majorana case, the two leptons may have the same charge. This should be the first visible channel if N is the lightest new particle and it mixes with one of the known lepton generations.

(B) $e^+e^- \to L^+L^-$ with a flavour-mixing decay into a light neutrino $L^- \to \nu_\ell W^-$:

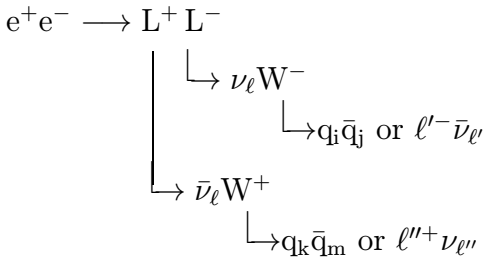

This process leads typically to multi-jet events with large transverse momentum or transverse missing energy. This should be the first visible channel if L^- is the lightest new particle and it mixes with one of the known lepton generations.

(C) $e^+e^- \to L^+L^-$ where $L^- \to NW^-$ (where N is a stable or long-lived neutral heavy lepton which decays outside the detector). This production is possible if N is the lighter member of an SU(2) doublet which does not mix with the lighter generations.

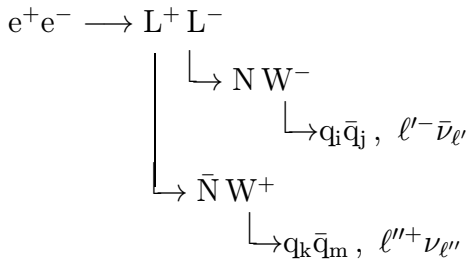

This signal leads to a very low visible energy if the mass difference, $M_{\mathrm{L}^\pm} - M_{\mathrm{N}}$, is small. This would be the signature of a naive fourth generation lepton doublet which does not mix appreciably with the three known lepton generations and which satisfies $M_{\mathrm{L}^\pm} > M_{\mathrm{N}}$.

For completeness, a final search should be performed looking for long-lived charged heavy leptons, which could come from a fourth generation with $M_{\mathrm{L}^\pm} < M_{\mathrm{N}}$ and very small mixing. The signature would be a pair of heavy charged particles visible in the detector. This topology will be included in a subsequent paper.

1.2 Excited Leptons

Excited leptons are new massive states of leptons expected in compositeness models. They are assumed to have the same electroweak SU(2) and U(1) gauge couplings to the vector bosons, g and g', as the Standard Model leptons, but are expected to be grouped into both left- and right-handed weak isodoublets with vector couplings. The existence of the right-handed doublets is required to protect the ordinary light leptons from radiatively acquiring a large anomalous magnetic moment via the $\ell^*\ell V$ interaction [18] (V is a γ, Z or $\mathrm{W}^\pm$ vector boson).

Excited leptons could be produced in pairs in $\mathrm{e}^+\mathrm{e}^-$ collisions via the process $\mathrm{e}^+\mathrm{e}^- \to \ell^*\bar{\ell}^*$, governed by the $\ell^*\ell^*V$ coupling. Depending on the details of the three $\ell^*\ell V$ couplings, they could be detected in photonic, CC or NC channels:

$$\nu^*_\ell \to \nu_\ell\gamma \quad , \quad \nu^*_\ell \to \ell^\pm\mathrm{W}^\mp \quad , \quad \nu^*_\ell \to \nu_\ell\mathrm{Z},$$

$$\ell^{*\pm} \to \ell^\pm\gamma \quad , \quad \ell^{*\pm} \to \nu_\ell\mathrm{W}^\pm \quad , \quad \ell^{*\pm} \to \ell^\pm\mathrm{Z},$$

where ν^* is a neutral excited lepton, $\ell^{*\pm}$ is a charged excited lepton, and $\ell = \mathrm{e}$, μ or τ.

The branching fractions of the excited leptons into the different vector bosons is determined by the strength of the three $\ell^*\ell V$ couplings, which also determine the size of the single-production cross-section. We use the effective Lagrangian [18]

$$\mathcal{L}_{\ell\ell^*} = \frac{1}{2\Lambda}\bar{\ell}^*\sigma^{\mu\nu}\left[gf\frac{\boldsymbol{\tau}}{2}\mathbf{W}_{\mu\nu} + g'f'\frac{Y}{2}B_{\mu\nu}\right]\ell_{\mathrm{L}} + \text{hermitian conjugate},$$

which describes the generalized magnetic de-excitation of the ℓ^* states. The matrix $\sigma^{\mu\nu}$ is the covariant bilinear tensor, $\boldsymbol{\tau}$ are the Pauli matrices, $\mathbf{W}_{\mu\nu}$ and $B_{\mu\nu}$ represent the fully gauge-invariant field tensors and Y is the weak hypercharge. The parameter Λ has units of energy and can be regarded as the "compositeness scale," while f and f' are couplings associated with the different gauge groups.

Depending on the relative values of f and f', at the mass scales within the sensitivity of LEP either the photonic or CC decay tends to have the largest branching fraction, and in this paper we will consider only these two decay modes. For simplicity, we will interpret our results using two example complementary coupling assignments, $f = f'$ and $f = -f'$.

Several analyses are used for the excited lepton search:

(A) $e^+e^- \to \nu^* \bar{\nu}^{(*)}$, with CC decays of the neutral excited lepton(s):

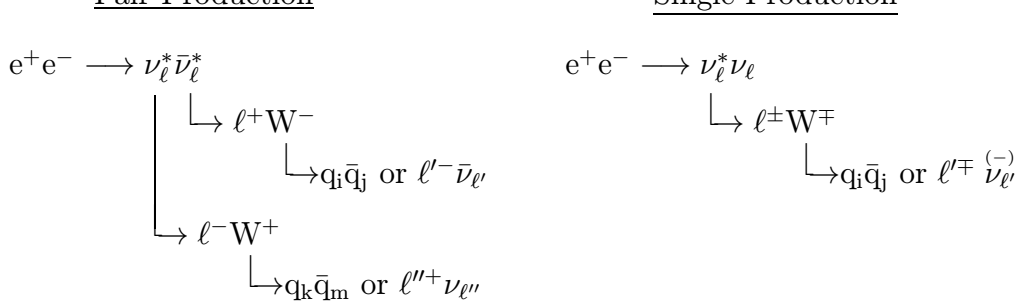

The topology of pair-production with CC decays is almost identical to the flavour-mixing decay of neutral heavy leptons considered as case (A) in Section 1.1, and the same analysis is used. The topology of single-production with CC decays can be categorised by the $W^\pm$ decay mode. If the $W^\pm$ decays leptonically, the signature is two leptons with missing transverse momentum (acoplanar lepton pair), while if it decays hadronically, the signature is an isolated lepton with two hadronic jets plus missing energy. In this latter case, the mass of the excited lepton can be reconstructed.

(B) $e^+e^- \to \ell^{*\pm} \ell^{(*)\mp}$, with CC decays of the charged excited lepton(s):

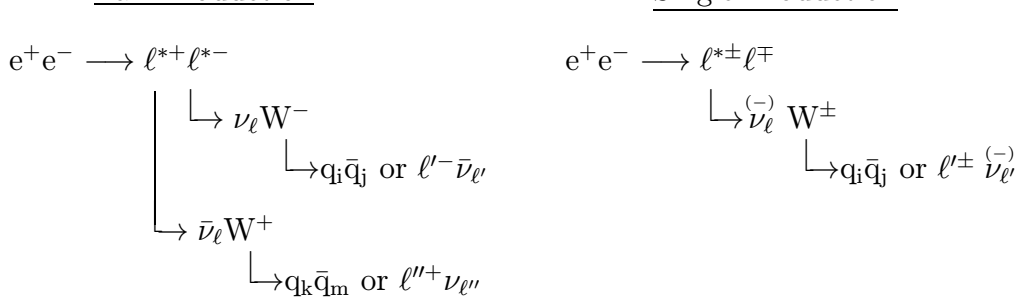

Again, the analysis for the flavour-mixing decay of charged heavy leptons considered as case (B) in Section 1.1 is used for pair-production. The topologies of single-production with CC decays are the same as that for neutral excited leptons, and the same analysis is used.

(C) $e^+e^- \to \nu^* \bar{\nu}^{(*)}$, with photonic decays of the neutral excited lepton(s):

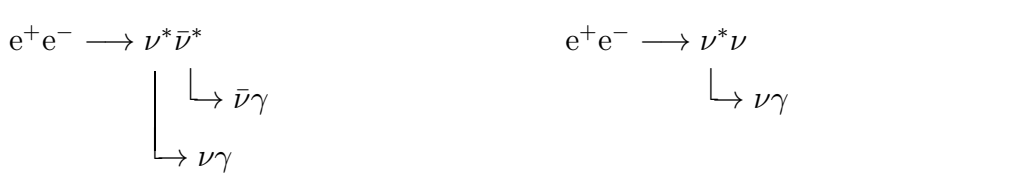

The signature is one or two photons plus significant missing energy. While no direct mass reconstruction is possible, the kinematics of the photon(s) can be used to restrict the excited neutrino mass which is consistent with the event.

(D) $e^+e^- \to \ell^{*\pm}\ell^{(*)\mp}$, with photonic decays of the charged excited lepton(s):

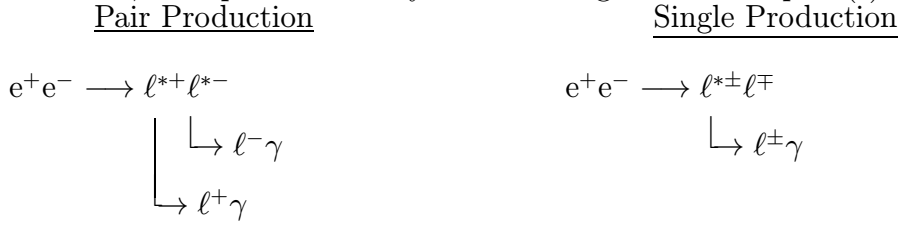

The signature is two leptons plus one or two photons with no missing energy, and the excited lepton mass can be reconstructed from the lepton-photon invariant mass. If the $e^*e\gamma$ coupling is significant, excited electron single-production is dominated by t-channel photon exchange; in this case, the recoil electron is most often missing along the beam axis, making a search in the $e\gamma$ plus missing electron topology interesting as well.

2 The OPAL Detector and Data Sample

A complete description of the OPAL detector can be found in Reference [19], and it is described only briefly here. The central detector consists of a system of tracking chambers that provides charged particle tracking over 96% of the full solid angle[1] inside a uniform 0.435 T magnetic field. It consists of a two-layer silicon microstrip vertex detector, a high-precision vertex drift chamber, a large-volume jet chamber and a set of z chambers that measures the track coordinates along the beam direction. The specific ionization energy loss per unit path length in the jet chamber, $\mathrm{d}E/\mathrm{d}x$, is used for particle identification. A lead-glass electromagnetic calorimeter located outside the magnet coil covers the full azimuthal range with excellent hermeticity in the polar angle range of $|\cos\theta| < 0.82$ for the barrel region and $0.81 < |\cos\theta| < 0.984$ for the endcap region. In the region where the barrel and endcap calorimeters overlap, photon and electron energy resolution is somewhat degraded because of extra material in front of the calorimeters. A set of wire-chambers in front of the electromagnetic calorimeter, the presampler, is used to measure the shape of electromagnetic showers from electrons and photons that interact in the magnet coil, and is used to aid electron identification. The magnet return yoke is instrumented with streamer tubes with cathode-strip readout for hadron calorimetry and consists of barrel and endcap sections along with pole-tip detectors that together cover the region $|\cos\theta| < 0.99$. Muons are identified with the hadron calorimeter strips, and with four layers of muon chambers which cover the outside of the hadron calorimeter. The gamma-catcher, forward-detector and silicon-tungsten electromagnetic calorimeters complete the geometrical acceptance down to 24 mrad. The silicon-tungsten calorimeter is used for the luminosity measurement.

The primary data sample used in this paper has an integrated luminosity of 1.0 pb^{-1} at $\sqrt{s} = 170.3$ GeV and 9.3 pb^{-1} at $\sqrt{s} = 172.3$ GeV and was acquired by OPAL during the

[1]The OPAL coordinate system is defined so that the z-axis is in the direction of the electron beam and the x-axis points towards the centre of the LEP ring; θ and ϕ are the polar and azimuthal angles, defined relative to the $+z$- and $+x$-axes, respectively.

autumn 1996 LEP running period. The results are combined with those obtained from 10.3 pb^{-1} of data at $\sqrt{s} = 161.3$ GeV acquired during the summer of 1996. The luminosities used in the purely photonic events selection are slightly different due to small differences in the detector status requirements used in those analyses.

3 Monte Carlo Simulation

A new Monte Carlo generator, EXOTIC, has been used for the simulation of $\mathrm{e^+e^-} \to \mathrm{N\bar{N}}$ and $\mathrm{e^+e^-} \to \mathrm{L^+L^-}$ events. The code is based on formulae given in references [16, 20] and the matrix elements include all spin correlations in the production and decay processes of the heavy leptons, and a complete treatment of the transition from 3-body to 2-body heavy fermion decays; it uses JETSET [21] for fragmentation and hadronization of quarks. For $\mathrm{N\bar{N}}$, and for $\mathrm{L^+L^-}$ with $\mathrm{L^-} \to \nu_\ell \mathrm{W^-}$, production, Monte Carlo samples of 2000 events each were generated for a set of masses in the region of sensitivity of this analysis. Different samples for Dirac- and Majorana-type heavy neutral leptons were generated, taking into account the different angular distributions in the two cases. For the case where $\mathrm{L^-} \to \mathrm{NW^-}$, samples of 1000 events each were simulated at 30 points in the (M_L,M_N) plane with M_L ranging from 70 to 85 GeV and M_N from 40 to 80 GeV, and with a mass difference $M_\mathrm{L} - M_\mathrm{N}$ larger than 5 GeV.

The excited lepton Monte Carlo samples were simulated with the existing generators EXLP and LSTAR described in Reference [9]. These generators use the formulae from Reference [18], but without taking into account the spin correlations in the production and decay of excited leptons. The effect of spin correlations on the efficiency for the detection of excited leptons has been studied using analytic approximations and also using EXOTIC, which supports excited leptons as well, and it was found to be negligible. For the pair production channels, samples of 2000 events each were generated for masses in the range from 65 to 85 GeV, and for the single production case samples of 2000 events each were generated for masses in the range from 80 to 170 GeV.

The backgrounds from Standard Model processes were studied with a variety of Monte Carlo generators. Two-fermion processes were simulated with BHWIDE [22] (large-angle Bhabha scattering), TEEGG [23] (t-channel Bhabha scattering), KORALZ [24] (muon- and tau-pair production) and PYTHIA [21] ($\mathrm{e^+e^-} \to \mathrm{Z}/\gamma \to \mathrm{q\bar{q}}$). These generators all include both initial- and final-state radiation, which is particularly important for the radiative decay analyses.

Hadronic two-photon processes of the form $\mathrm{e^+e^-} \to \mathrm{e^+e^-q\bar{q}}$, with the final-state electrons scattered at small angles, were simulated with PYTHIA, HERWIG [25] and PHOJET [26]. Leptonic two-photon processes were simulated with Vermaseren [27]. Other 4-fermion processes, the most important of which is $\mathrm{W^+W^-}$ production, were studied with PYTHIA, FERMISV [28], EXCALIBUR [29] and grc4f [30]. FERMISV simulates neutral-current 4-fermion processes, which can be combined with $\mathrm{W^+W^-}$ production samples generated with PYTHIA. EXCALIBUR and grc4f include CC and NC 4-fermion processes and all interference effects. Different combinations of samples from the different 4-fermion generators yielding a complete estimate of the background processes gave consistent predictions.

Finally, Standard Model processes with only photons in the final state are an important

background to the analysis of excited neutral leptons with photonic decays. The RADCOR [31] program was used to simulate the process $e^+e^- \to \gamma\gamma(\gamma)$, and both KORALZ and NUNUGPV [32] were used to simulate the process $e^+e^- \to \nu\overline{\nu}\gamma(\gamma)$.

All signal and background Monte Carlo samples were processed through the full OPAL detector simulation [33], and passed through the same analysis chain as the data.

4 Selection Criteria

Since the searches presented in this paper involve many different experimental topologies, a number of different analyses are used for the heavy and excited lepton searches. These analyses evolved independently and use slightly different criteria for such details as track and cluster quality requirements and lepton identification methods. In Section 4.1, the three analyses for the CC decays of pair-produced heavy and excited leptons are described. Next, Section 4.2 details the search for the single production of neutral and charged excited leptons with CC decays. Section 4.3 summarizes the search for neutral excited leptons with photonic decays. Finally, in Section 4.4, the selection of charged excited leptons with photonic decays is described.

4.1 Pair Production of Heavy Leptons and of Excited Leptons with CC Decays

All charged tracks and calorimeter clusters are subjected to some quality criteria: each track is required to have a minimum momentum transverse to the beam axis, p_{T}, of 0.15 GeV, to have a minimum number of 20 hits in the central tracking detector, and to point to the geometrical centre of the detector to within 2 cm and to pass within 25 cm of the origin in z at the point of closest approach in $r\phi$; each electromagnetic cluster in the barrel is required to have a minimum energy of 0.1 GeV, while for the endcap regions the minimum raw energy is 0.25 GeV; hadronic clusters are required to have a minimum energy of 0.25 GeV. In calculating the total visible energy and momentum of events, and of individual jets, corrections are applied which reduce the effects of the double-counting of energy from tracks and clusters associated to them [34]. Jet reconstruction is done by using the $k_\perp$ ("Durham") [35] jet-finding algorithm with a resolution parameter y_{cut} of 0.004. For electron, muon, and tau identification the following procedures are applied:

electron: a track is identified as an electron candidate if at least one of the following two methods is satisfied.

1. A standard electron identification: each good charged track in the central detector, which satisfies all the following criteria, is considered as an electron candidate:
   - $p > 3.0$ GeV, where p is the track momentum.
   - $0.7 < E/p < 1.4$, where E is the energy of the electromagnetic cluster associated to the track.

- $8 < \mathrm{d}E/\mathrm{d}x < 13$ keV/cm, where $\mathrm{d}E/\mathrm{d}x$ is the ionization energy loss per unit path length measured in the central detector.
- the number of $\mathrm{d}E/\mathrm{d}x$ measurements is at least 20.

2. The output of an artificial neural network designed to identify electrons [36] is required to exceed 0.90. The network uses information mainly from the track momentum, $\mathrm{d}E/\mathrm{d}x$, the energy in the associated electromagnetic calorimeter cluster, the number of lead-glass blocks in the cluster, and the presampler signal associated with the track.

In each case there is an isolation requirement on the electron candidate using the total energy in a cone of half-opening angle 15° surrounding the electron, excluding the energy of the electromagnetic cluster associated with the candidate. The electron is considered to be isolated if this energy does not exceed 5 GeV.

muon: a track with $p > 3.0$ GeV is identified as a muon candidate if it is matched with track segments in the muon chambers. In regions not covered by the muon chambers the identification is done by using a match with the hadron calorimeter strips. We require that muon candidates be isolated as described above for electrons.

tau: a tau lepton candidate is selected by either the electron or muon identification (as above) for a 1-prong tau decay into an isolated lepton (e or μ), or by jet reconstruction for a 1-prong or a 3-prong tau decay into hadrons. A jet is identified as a tau if either of the following criteria were satisfied.

1. for a 1-prong decay, all of the following conditions must be satisfied:
   - it contained at least 1 track with $p > 3.0$ GeV.
   - no track was found within a cone of half-opening angle 15° surrounding the track.
   - the momentum sum of the other tracks within the jet was less than 1.0 GeV.
   - the invariant mass of all tracks and clusters within the cone was less than 3.0 GeV.
2. for a 3-prong decay, all of the following conditions must be satisfied:
   - it contained exactly 3 tracks in a cone of half-opening angle 15° around the jet axis.
   - the momentum sum of the 3 tracks was greater than 3.0 GeV.
   - the invariant mass of all tracks and clusters within the cone was less than 3.0 GeV.

4.1.1 Selection of N$\bar{\mathrm{N}}$ Candidates

To be considered as potential candidates for N$\bar{\mathrm{N}}$, or $\nu^*\bar{\nu}^*$ with CC decays (category A in Section 1.1, and pair-production for category A in Section 1.2), the events must pass the following set of cuts:

1. A standard multihadronic selection where tracks and energy clusters satisfy the following (good tracks and clusters are those which satisfy the quality criteria defined in Section 4.1):

   - $R_{\rm vis} \geq 0.10$, where $R_{\rm vis} = \frac{E_{\rm shw}}{2\times E_{\rm beam}}$; $E_{\rm shw} = \sum E_{\rm raw}$ and $E_{\rm raw}$ is the raw energy of a good cluster and $E_{\rm beam}$ is the beam energy.
   - $R_{\rm bal} \leq 0.65$, where $R_{\rm bal} = \frac{E_{\rm bal}}{E_{\rm shw}}$; $E_{\rm bal} = \sum E_{\rm raw} \cos\theta$ (θ is the polar angle of the cluster).
   - there are at least 7 good clusters.
   - there are at least 5 good tracks.

2. There are at least 2 isolated leptons of the same flavour (e, μ, or τ). We do not apply a charge constraint in order to be sensitive both to Dirac and Majorana neutral heavy leptons.

3. To reject radiative events, principally $e^+e^- \to Z\gamma$ with the photon missing along the beam axis, we require that $|\cos\theta_{\rm miss}| < 0.95$ if $E_{\rm miss} > 35$ GeV, where $\theta_{\rm miss}$ is the angle between the missing energy vector and the beam axis and $E_{\rm miss}$ is the missing energy in the event (the most probable photon energy from $e^+e^- \to Z\gamma$ is about 60 GeV). The distributions after cut 2 of $|\cos\theta_{\rm miss}|$ versus $E_{\rm miss}$ are shown in Figures 1(a) and 1(b).

4. The number of reconstructed jets is required to be at least four. The distributions after cut 3 of the numbers of reconstructed jets are shown in Figure 1(c).

5. For the case $N \to \tau W$ an extra cut is applied to reduce the larger background: we require that $65 < E_{\rm vis} < 160$ GeV, where $E_{\rm vis}$ is the visible energy. The visible energy distributions after cut 4 are shown in Figure 1(d).

For the cases $N \to eW$ and $N \to \mu W$ the remaining numbers of events after each cut are displayed in Tables 1 and 2 respectively (numbers for Dirac- and Majorana-type N signals are shown in the same table). The numbers of events remaining for $N \to \tau W$ after each cut are displayed in Table 3.

The efficiencies obtained for the $N\bar{N}$ and $\nu^*\bar{\nu}^*$ selections after applying the full analysis are evaluated from the Monte Carlo samples discussed in Section 3. The efficiencies are about 60% for $N \to eW$, 50% for $N \to \mu W$, and 30% for $N \to \tau W$.

4.1.2 Selection of L^+L^- Candidates with $L^- \to \nu_\ell W^-$

In order to be considered as potential candidates for L^+L^-, or $\ell^{*+}\ell^{*-}$ with CC decays, where each charged heavy lepton decays into a light standard neutrino (category B in Section 1.1, and pair-production for category B in Section 1.2), the events must satisfy the following set of selection criteria:

1. The same multihadronic selection as cut 1 in Section 4.1.1.

After Cut	Data	Total Bkg	$q\bar{q}(\gamma)$	two-photon	$\tau\tau(\gamma)$	4-f	Dirac $M_N = 75$ GeV	Majorana $M_N = 65$ GeV
Presel	–	–	–	–	–	–	6.26	4.59
1	1411	1288	1137	26.6	3.33	120.8	5.67	4.15
2	1	1.72	0.35	0.0	0.03	1.34	4.07	3.14
3	1	1.48	0.21	0.0	0.03	1.25	4.01	3.07
4	0	0.68	0.08	0.0	0.01	0.59	3.88	2.89

Table 1: Observed number of events in the data sample and expected number of events from the background sources and the $N\bar{N}$ signal (Dirac- and Majorana-types) for the case where $N \to eW$, normalized to the actual integrated luminosity at $\sqrt{s} = 172$ GeV. The statistical error on the background Monte Carlo is small compared to that for data.

After Cut	Data	Total Bkg	$q\bar{q}(\gamma)$	two-photon	$\tau\tau(\gamma)$	4-f	Dirac $M_N = 75$ GeV	Majorana $M_N = 65$ GeV
Presel	–	–	–	–	–	–	6.26	4.59
1	1411	1288	1137	26.6	3.33	120.8	5.37	3.81
2	0	1.23	0.27	0.0	0.0	0.96	3.41	2.53
3	0	1.02	0.13	0.0	0.0	0.89	3.37	2.47
4	0	0.51	0.04	0.0	0.0	0.47	3.28	2.36

Table 2: Observed number of events in the data sample and expected number of events from the background sources and the $N\bar{N}$ signal (Dirac- and Majorana-types) for the case where $N \to \mu W$, normalized to the actual integrated luminosity at $\sqrt{s} = 172$ GeV. The statistical error on the background Monte Carlo is small compared to that for data.

After Cut	Data	Total bkg	$q\bar{q}(\gamma)$	two-photon	$\tau\tau(\gamma)$	4-f	Dirac $M_N = 65$ GeV	Majorana $M_N = 55$ GeV
Presel	–	–	–	–	–	–	10.05	8.25
1	1411	1288	1137	26.6	3.33	120.8	9.42	7.62
2	4	7.99	2.44	0.59	0.10	4.84	3.68	2.86
3	4	6.53	1.41	0.48	0.09	4.52	3.62	2.81
4	3	3.52	0.61	0.48	0.02	2.40	3.26	2.45
5	2	1.98	0.21	0.0	0.01	1.76	3.05	2.26

Table 3: Observed number of events in the data sample and expected number of events from the background sources and the $N\bar{N}$ signal (Dirac and Majorana types) for the case where $N \to \tau W$, normalized to the actual integrated luminosity at $\sqrt{s} = 172$ GeV. The statistical error on the background Monte Carlo is small compared to that for data.

After Cut	Data	Total Bkg	$q\bar{q}(\gamma)$	two-photon	$\tau\tau(\gamma)$	4-f	L^+L^- $M_L = 80$ GeV
Presel	–	–	–	–	–	–	14.7
1	1411	1288	1137	26.6	3.33	120.8	12.5
2	1044	990.3	866.5	11.2	2.84	109.9	11.5
3	406	398.8	303.7	3.60	1.71	89.8	10.1
4	133	129.6	70.4	1.65	0.23	57.3	7.4
5 or 6	1	3.07	0.78	0.0	0.01	2.28	3.2

Table 4: Observed number of events in the data sample and expected number of events from the background sources and the L^+L^- signal for the case where $L^- \to \nu_\ell W^-$, normalized to the actual integrated luminosity at $\sqrt{s} = 172$ GeV. The statistical error on the background Monte Carlo is small compared to that for data.

2. To reduce the background from $q\bar{q}(\gamma)$ and two-photon processes we require that the energy deposited in each forward-calorimeter, each gamma-catcher, and each silicon-tungsten calorimeter be less that 2 GeV, 5 GeV, and 5 GeV, respectively.

3. Non-radiative events are selected by demanding that $|\cos\theta_{\rm miss}| < 0.85$. The $|\cos\theta_{\rm miss}|$ distributions after cut 2 are shown in Figure 2(a).

4. To reject events containing two back-to-back jets mostly from $q\bar{q}(\gamma)$, the thrust of the event was required to be less than 0.85. The thrust distributions after cut 3 are shown in Figure 2(b).

5. If no isolated lepton is found in the event we apply the following constraints:

   - $80 < E_{\rm vis} < 145$ GeV. The visible energy distributions after cut 4 are shown in Figure 2(c).
   - $p_{\rm Tmiss} > 15$ GeV, where $p_{\rm Tmiss}$ is the missing momentum transverse to the beam axis. The distributions for $p_{\rm Tmiss}$ after cut 4 are shown in Figure 2(d).
   - $N_{\rm jets} \geq 4$, where $N_{\rm jets}$ is the number of reconstructed jets.
   - the maximum momentum of the good tracks should not exceed 25 GeV.

6. If one or more isolated lepton is found, we apply the following cuts:

   - $E_{\rm vis} < 100$ GeV. The visible energy distributions after cut 4 are shown in Figure 2(e).
   - $p_{\rm Tmiss} > 20$ GeV. The distributions for $p_{\rm Tmiss}$ after cut 4 are shown in Figure 2(f).
   - $N_{\rm jets} \geq 3$.

The remaining numbers of events after each cut are displayed in Table 4. The efficiencies obtained after all cuts are estimated from Monte Carlo to be 20–25%, depending on the mass of the heavy or excited lepton.

4.1.3 Selection of L^+L^- Candidates with $L^- \to NW^-$

To be considered as potential L^+L^- candidates, where the charged heavy lepton decays into a stable neutral heavy lepton (category C in Section 1.1), the events must satisfy the following set of cuts. Here we do not use the standard selection of multihadronic events since for small mass differences, $M_L - M_N$, the visible energy is very low and the particle multiplicity is small.

1. We require at least 5 good charged tracks.
2. The criteria for energy deposited in the forward-detector, the gamma-catcher, and the silicon-tungsten calorimeter are the same as in Section 4.1.2.
3. In order to reduce background from beam-gas and beam-wall interactions we require that $|\cos\theta_{\rm thrust}|$ be smaller than 0.9, where $\theta_{\rm thrust}$ is the polar angle of the thrust axis. The $|\cos\theta_{\rm thrust}|$ distributions after cut 2 are shown in Figure 3(a).
4. To reduce the large background coming from two-photon processes, we apply a cut on the missing momentum transverse to the beam axis: $p_{\rm Tmiss} > 5$ GeV (including clusters from the hadronic calorimeter), and $p_{\rm Tmiss}^{\rm no-HCAL} > 5$ GeV (excluding hadronic calorimeter clusters). The $p_{\rm Tmiss}$ distributions after cut 3 are shown in Figure 3(b).
5. For radiative-event rejection we require that $|\cos\theta_{\rm miss}| < 0.7$. The $|\cos\theta_{\rm miss}|$ distributions after cut 4 are shown in Figure 3(c).
6. The two heavy neutrinos coming from L^+ and L^- carry away a significant fraction of the energy. To reduce the background from multihadronic and four-fermion events, we require that $E_{\rm vis} < 75$ GeV. The $E_{\rm vis}$ distributions after cut 5 are shown in Figure 3(d).
7. Four-fermion processes and $\tau\tau$ backgrounds were reduced by requiring that the maximum momentum of a good track should not exceed 20 GeV. The distributions of $p_{\rm max}$ after cut 6 are shown in Figure 3(e).
8. We require that the thrust value be less than 0.9 in order to reject events containing two back-to-back jets. The distributions of the thrust after cut 7 are shown in Figure 3(f).

The remaining numbers of events after each cut are displayed in Table 5. The total selection efficiencies are typically 40–50%, but drop to 9–12% for $M_L - M_N \sim 5$ GeV.

4.2 Single Production of Excited Leptons with Charged Decays

Two searches are performed for the charged decays of singly-produced excited leptons (single-production for categories A and B in Section 1.2). The first analysis looks only for leptonic decays of the $W^\pm$, which may be real or virtual depending on the mass of the ν^*. The topology is then $e^+e^- \to \nu_\ell^*\nu_\ell \to \nu_\ell\ell^\pm W^\mp \to \nu_\ell\ell^\pm\nu_{\ell'}\ell'^\mp$, where $\ell^\pm$ corresponds to the excited lepton flavour, and $\ell'^\mp$ may or may not be of the same flavour. Since charged excited leptons with charged decays, $e^+e^- \to \ell^{*\pm}\ell^\mp \to \nu_\ell\ell^\mp W^\pm \to \nu_\ell\ell^\mp\nu_{\ell'}\ell'^\pm$, can have the same final states as

After Cut	Data	Total Bkg	$q\bar{q}(\gamma)$	two-photon	$\tau\tau(\gamma)$	4-f	L^+L^-	
							$M_L = 75$ GeV $M_N = 60$ GeV	$M_L = 80$ GeV $M_N = 50$ GeV
Presel	–	–	–	–	–	–	21.52	14.69
1	40935	41602	1242	40223	9.30	125.3	17.82	12.84
2	19792	21753	908.5	20725	8.02	112.1	17.30	12.34
3	8258	8098	819.4	7165	7.10	106.2	15.90	11.45
4	531	477.1	382.6	7.41	5.16	81.8	13.36	10.65
5	211	200.6	135.81	2.04	2.60	60.2	11.15	8.44
6	6	3.87	1.10	1.97	0.42	0.39	11.15	8.30
7	3	3.35	1.08	1.73	0.27	0.28	11.15	7.91
8	1	1.90	0.56	1.12	0.06	0.16	10.33	7.35

Table 5: Observed number of events in the data sample and expected number of events from the background sources and the L^+L^- signal for the case where $L^- \to NW^-$, normalized to the actual integrated luminosity at $\sqrt{s} = 172$ GeV. The statistical error on the background Monte Carlo is small compared to that for data.

neutral excited leptons with charged decays, the same search is used. The topology is a pair of leptons which are not coplanar with the beam direction.

The second search for the charged decays of singly-produced excited leptons is optimised for the hadronic decays of the $W^\pm$ boson, looking in the $e^+e^- \to \nu_\ell^* \nu_\ell \to \nu_\ell \ell^\pm W^\mp \to \nu_\ell \ell^\pm q_i \overline{q}_j$ channels. In this search, we look only in the electron and muon channels; the high background levels in the tau channel do not allow improvement over the sensitivity of the acoplanar lepton pair analysis. Since charged excited leptons with charged decays, $e^+e^- \to \ell^{*\pm}\ell^\mp \to \nu_\ell \ell^\mp W^\pm \to \nu_\ell \ell^\mp q_i \overline{q}_j$, can have the same final states as neutral excited leptons with charged decays, the same search is used.

4.2.1 Acoplanar Lepton Pair Analysis

Using the same preselection and track quality cuts as the $\ell^+\ell^-\gamma(\gamma)$ analysis in Section 4.4, candidate $\ell^{*\pm}$ and ν_ℓ^* events are required to satisfy the following criteria:

1. There must be exactly two identified leptons, at least one of type $\ell^\pm$ corresponding to the excited lepton flavour. At least one of the leptons must have an energy greater than $0.2E_{\rm beam}$.

2. There must be no other track passing the quality cuts in the event.

3. Excluding the clusters associated with the two leptons, the sum of other barrel and endcap electromagnetic calorimeter cluster energies must be less than 10 GeV.

4. Events from two-photon processes are suppressed by requiring that the energy deposited in each forward-calorimeter, each gamma-catcher and each silicon-tungsten calorimeter be less than 2 GeV, 5 GeV and 5 GeV, respectively.

Topology	After Cut	Data	Total Bkg	$\ell^{*\pm}\ell^{\mp}$		$\nu^*\nu$	
				$M_* =$ 80 GeV	$M_* =$ 140 GeV	$M_* =$ 80 GeV	$M_* =$ 140 GeV
eℓ	1	1377	1344.3	23.7	23.4	20.5	23.8
	2	1356	1330.8	23.3	23.3	20.1	23.6
	3	1297	1272.7	22.0	23.0	19.2	23.4
	4	1208	1202.1	20.3	22.3	18.7	23.2
	5	852	833.0	18.9	20.4	17.9	21.4
	6	3	4.7	14.8	18.2	16.9	19.8
$\mu\ell$	1	192	189.8	25.7	26.5	22.3	25.3
	2	185	184.1	25.3	26.3	22.1	25.2
	3	163	156.0	23.5	26.0	20.6	24.7
	4	136	129.0	22.1	25.5	18.9	24.3
	5	50	55.7	20.0	24.2	17.9	22.0
	6	3	5.0	14.4	21.6	17.0	19.9
$\tau\ell$	1	1646	1621.6	21.2	18.8	14.8	22.9
	2	1623	1603.5	20.9	18.7	14.6	22.9
	3	1536	1513.7	19.6	18.4	13.5	22.6
	4	1415	1407.8	18.3	18.0	12.5	22.2
	5	930	913.6	16.5	16.7	12.0	20.8
	6	4	7.5	12.5	14.7	11.2	19.1

Table 6: Number of events surviving each cut, and selection efficiencies in percent, in the search for the single production of $\ell^{*\pm}$ and ν^* with charged decays in the acoplanar di-lepton channel. The background Monte Carlo sum is normalized to the actual integrated luminosity at $\sqrt{s} = 172$ GeV. The three selections are not independent; in particular, the $\tau\ell$ selection completely includes both the eℓ and $\mu\ell$ selections. The efficiencies include the leptonic branching ratio of the W. The statistical error on the background Monte Carlo is small compared to that for data.

5. Events with missing momentum along the beam axis are removed by requiring $|\cos\theta_{\rm miss}| < 0.9$, where $\theta_{\rm miss}$ is the polar angle of the missing momentum.

6. Events are required to be acoplanar by requiring $\phi_{\ell\ell}^{\rm ACOP} > 20^\circ$ ($\phi_{\ell\ell}^{\rm ACOP}$ is 180° minus the opening angle between the two leptons in the x-y plane). The acoplanarity angle is plotted for the excited electron, muon and tau search in Figures 4(a), (b) and (c), respectively.

The complete analysis is summarized in Table 6. The numbers of events selected in each channel are consistent with the expectations from Standard Model sources. After cut 6, the dominant background is from $\rm W^+W^-$ production. The total selection efficiencies for excited lepton single production with CC decays when the $\rm W^\pm$ decays leptonically is about 55% for $\rm e^*$, $\nu_{\rm e}^*$, μ^* and ν_μ^*, and about 45% for τ^* and ν_τ^*.

4.2.2 $\ell^{\pm}\nu q\bar{q}$ Analysis

All charged tracks and calorimeter clusters are subjected to the same quality criteria used in the unstable heavy lepton analysis in Section 4.1. As in that section, overlap between tracks and clusters is also corrected using the method described in Reference [34]. A preselection is used to remove low multiplicity events. At least six tracks passing the quality cuts must be reconstructed in an event, the ratio of the number of selected tracks to the total number of reconstructed tracks must be greater than 0.2, and at least 8 clusters must be reconstructed in the event. Following the preselection, candidate events are required to satisfy the following criteria:

1. There must be at least one isolated lepton ℓ (ℓ = e or μ), corresponding to the excited lepton flavour. The reconstructed track corresponding to the lepton candidate should lie within the angular region $|\cos\theta| < 0.95$. Leptons consistent with coming from a Z decay are rejected if their invariant mass when combined with any other track is within 10 GeV of the Z mass. If there is more than one lepton candidate, then the candidate with the highest momentum is taken. The lepton must satisfy one of the following criteria:

   electron: A track is identified as an electron if it satisfies either of the following criteria:

   (a) The track must be associated with an electromagnetic calorimeter cluster with a minimum energy of 2.0 GeV. The sum of the magnitudes of the momenta of tracks and energy of unassociated electromagnetic clusters in a cone with half-angle of 15° around the electron track should be less than 2.5 GeV. Candidate electron tracks with $|\cos\theta| < 0.79$ or $|\cos\theta| \geq 0.815$, are required to satisfy $E/p > 0.7$. Candidate electron tracks with $0.79 \leq |\cos\theta| < 0.815$ should satisfy $E/p > 0.5$. The $\mathrm{d}E/\mathrm{d}x$ energy loss of tracks must be consistent with that expected from an electron.

   (b) The output of a neural network electron finder [36] must be greater than 0.8.

   muon: A track with $p > 2$ GeV is identified as a muon if it is matched with track segments in the muon chambers. In regions not covered by the muon chambers the identification is done by using the hadron calorimeter strips.

2. To remove events from two-photon processes, events having significant energy in either side of the forward detectors are rejected. The maximum energy allowed in the gamma catcher is 5 GeV, in the forward calorimeter 2 GeV, and in the silicon tungsten detector is 2 GeV.

3. To reduce further two-photon events, the ratio of total visible energy of the event to the centre-of-mass energy, defined as $R_{\mathrm{vis}} = E_{\mathrm{vis}}/\sqrt{s}$, is required to be greater than 0.3. R_{vis} is plotted before this cut in Figure 5(a).

4. To reject events with initial state radiation along the beam axis, the missing energy vector of the event must satisfy $|\cos\theta_{\mathrm{miss}}| < 0.9$; $\cos\theta_{\mathrm{miss}}$ is plotted before the cut in Figure 5(b).

5. To suppress further the background from hadronic Z decays, the thrust of the event must be less than 0.95.

Topology	After Cut	Data	Total Bkg	$\ell^{*\pm}\ell^{\mp}$		$\nu^*\nu$	
				$M_* =$ 80 GeV	$M_* =$ 140 GeV	$M_* =$ 80 GeV	$M_* =$ 140 GeV
eq$\bar{\text{q}}$	1	449	403.3	59.4	64.8	59.7	61.2
	2	271	264.2	52.5	60.0	55.5	57.0
	3	223	233.6	52.1	60.0	55.5	57.0
	4	119	119.7	42.8	54.3	52.0	53.7
	5	98	96.5	39.6	54.0	51.5	51.9
	6	45	38.0	31.8	53.7	51.2	50.8
	7	7	4.4	15.2	23.2	30.8	22.0
μq$\bar{\text{q}}$	1	103	114.6	51.8	52.4	49.5	52.2
	2	45	57.8	45.8	48.2	44.3	48.6
	3	30	36.2	45.6	48.2	44.2	48.6
	4	20	23.2	35.9	43.8	37.1	44.6
	5	18	21.6	34.6	43.6	36.7	43.6
	6	9	12.9	27.6	43.4	35.8	43.2
	7	1	0.6	14.4	18.4	20.9	18.0

Table 7: Number of events surviving after each cut, and the selection efficiencies in percent, in the search for the single-production of $\ell^{*\pm}$ and ν^* with CC decays in the lepton plus jets and missing energy analysis. The background Monte Carlo sum is normalized to the actual integrated luminosity at $\sqrt{s} = 172$ GeV. The efficiency includes the hadronic branching ratio of the W. The statistical error on the background Monte Carlo is small compared to that for data.

6. The event is required to have a large missing momentum, p_{Tmiss}, or a large lepton energy, p_ℓ, with respect to the beam energy, E_{beam}. This is achieved by requiring $(p_{\text{Tmiss}} + p_\ell)/E_{\text{beam}} > 0.4$. p_{Tmiss} *vs.* p_ℓ is plotted before this cut in Figure 5(c). While only one example mass for an ℓ^* signal is shown in the figure, this cut retains high efficiency for all ℓ^* masses.

7. To reduce the contribution from W-pair production, the lepton candidate is removed from the event and the event is forced into two jets, using the Durham jet algorithm. The resulting invariant masses $m_{\ell-\text{miss}}$ and $m_{\text{jet}-\text{jet}}$ are required to satisfy:

   - $m_{\ell-\text{miss}} > 5$ GeV and $m_{\text{jet}-\text{jet}} < 95$ GeV,
   - $m_{\ell-\text{miss}} + m_{\text{jet}-\text{jet}} < 145$ GeV.

   $m_{\ell-\text{miss}}$ *vs.* $m_{\text{jet}-\text{jet}}$ is plotted before this cut in Figure 5(d).

The complete analysis is summarized in Table 7. The numbers of events selected in each channel are consistent with the expectation from Standard Model sources. The total selection efficiency for excited lepton single production with CC decays when the $\text{W}^\pm$ decays hadronically is typically from 20–45%, depending on the mass of the excited lepton, but drops to about 10% for ν^* near the kinematic limit.

No signal is observed. The results from both the acoplanar lepton pair and $\ell^\pm\nu\text{q}\bar{\text{q}}$ analyses are combined to infer limits on excited lepton single production with CC decays. The $\ell^\pm\nu\text{q}\bar{\text{q}}$

results include a $\pm$ 3 σ mass window, where σ is the average mass resolution determined from Monte Carlo, to classify each event as being consistent with an excited lepton in some mass range, while the selected acoplanar lepton pair events are considered as candidates for all excited lepton masses.

4.3 Production of Neutral Excited Leptons with Photonic Decays

The search for excited neutrino production with photonic decays (category C in Section 1.2) uses the OPAL analysis of photonic events with missing energy [37]. That analysis has one method optimised for events with one photon plus missing energy and another method optimised for events with two photons plus missing energy. These are used for the excited neutrino single- and pair-production searches, respectively. The search results for the full $\sqrt{s}$ = 161–172 GeV data set are summarized in Table 8; these selections have improved sensitivity over our previously published analyses [11], and are therefore used to update our $\sqrt{s}$ = 161 GeV results as well.

The search for a single photon plus missing energy selects events with either a single, energetic isolated cluster in the electromagnetic calorimeter, or an identified photon conversion, along with no other significant energy in the event. One event is selected at $\sqrt{s}$ = 161 GeV and another at $\sqrt{s}$ = 172 GeV, with a combined expected background of 0.7 to 0.8 events from Standard Model processes. There is a discrepancy of about 15% between the predictions of the expected background level to this analysis from the KORALZ and NUNUGPV generators, and we use the smaller number when performing limit calculations. The search for a photon pair plus missing energy selects events with two photon candidates, along with no other significant energy in the event. One event is selected at $\sqrt{s}$ = 161 GeV, and two more events are selected at $\sqrt{s}$ = 172 GeV, with an expected background from 4.7 to 9.2 events from Standard Model processes. In the photon pair topology, the discrepancy between KORALZ and NUNUGPV is much more serious, and no background subtraction is performed. As described in Reference [37], the kinematics of the photons are used to classify the events as being consistent with excited neutrino pair-production up to a maximum mass, $M^{\max}$. The maximum excited neutrino mass consistent with any of the three events is 69.7 GeV. While the events are taken as candidates, the excited neutrino masses with which they are consistent are sufficiently low that they do not affect the limits inferred from these data.

The total selection efficiency for photonic decays of pair-produced excited neutrinos is about 80%, and for singly-produced excited neutrinos varies from about 20–80% for excited neutrino masses of 80–170 GeV. The selection efficiency for singly-produced excited electron-neutrinos is slightly different than for excited muon- and tau-neutrinos because of the t-channel $W^{\pm}$-exchange contribution to the production angular distribution.

4.4 Production of Charged Excited Leptons with Photonic Decays

The single- and pair-production of excited leptons with photonic decays leads to $\ell^+\ell^-\gamma(\gamma)$ topologies (category D in Section 1.2). To be considered in the analysis, tracks in the central detector and clusters in the electromagnetic calorimeter must satisfy the normal quality criteria

Topology	Requirements	Data	NUNUGPV	KORALZ
1 γ	Single γ selection	85	94.7	92.6
	$M_{\rm miss} < 75$ GeV	3	1.7	1.9
	Remove poorly measured regions	2	0.8	0.7
2 γ	Two γ selection	3	9.2	4.7

Table 8: Number of events surviving in the two photonic events topologies at $\sqrt{s}$ = 161–172 GeV. The Standard Model background is completely dominated by $\nu\bar{\nu}\gamma\gamma$, and predictions from both the NUNUGPV and KORALZ generators are shown. The analyses and requirements used in new particle searches are discussed in detail in Reference [37]. The statistical error on the background Monte Carlo is small compared to that for data.

employed in the analysis of lepton pairs [38]. In addition, a "good" track must satisfy $|\cos\theta| < 0.95$.

A pre-selection is performed to remove obvious background events. Cosmic rays are rejected using timing and tracking information as described in the analysis of lepton pairs [38]. Residual beam-gas and beam-wall collision events are rejected by requiring that the fraction of good to total charged tracks reconstructed in the central detector be greater than 0.2. Background from multihadronic events is reduced by requiring that the number of good tracks (after removing tracks identified as part of photon conversions as described below) satisfies $N_{\rm trk} \leq 4$. The pre-selection also requires a minimum of one lepton candidate (electron, muon, or tau) and a minimum of one photon candidate, in the event, using the criteria defined below.

Tracks with $p_{\rm T} > 1$ GeV are considered as potential lepton candidates, and the following identification requirements are made:

electron: A track is identified as an electron if it satisfies any one of the following three criteria:

1. $0.8 < E/p < 1.3$, where p is the momentum of the track and E is the energy of the associated electromagnetic cluster.
2. $0.5 < E/p < 2.0$ and the signed $\mathrm{d}E/\mathrm{d}x$ weight [39] is consistent with the track being an electron.
3. The output of the electron identification neural network described in Reference [36] is greater than 0.8. This final criterion is desirable to recover some extra efficiency for low-energy recoil electrons in the single-production search.

The energy, $E_{\rm e}$, of the electron is computed using the electromagnetic calorimeter cluster energy and its direction is computed using the track observed in the central detector.

muon: A track is identified as a muon if it satisfies either of the following two criteria:

1. The track is identified as a muon according to the criteria employed in the analysis of Standard Model muon pairs [38]; that is, it has associated activity in the muon chambers or hadron calorimeter strips or it has a high momentum but is associated with only a small energy deposit in the electromagnetic calorimeter.

2. The track is identified as a muon according to the criteria employed in the analysis of muons in multihadronic events given in Reference [40]. This second criterion is desirable to recover some extra efficiency for low-energy recoil muons in the single-production search.

tau: a track is identified as originating from a tau decay if it satisfies either of the following two conditions:

1. It is identified as an electron or muon according to the above requirements (i.e. electrons and muons are also used as tau candidates).
2. There are at most two additional tracks in a cone with a half-angle of 20° around the track.

A tau "jet" is constructed by adding the momenta of all tracks and clusters inside the 20° half-angle cone. The energy of the tau jet is calculated using only the tracks in the central detector and energy in the electromagnetic calorimeter, correcting for double-counting using the method described in Reference [34].

A separate search is performed to identify photons:

photon: A photon candidate must satisfy either of the following two criteria:

1. An electromagnetic cluster with no associated good charged tracks.
2. A photon conversion identified with the algorithm employed in the analysis of muon pairs [38]. The tracks and clusters associated with the conversion are combined to form a single 4-vector representing the photon.

The photon is also required to satisfy $|\cos\theta| < 0.95$ and to have an energy greater than 1 GeV.

4.4.1 $\ell\ell\gamma\gamma$ Final States

Candidate $\ell^+\ell^-\gamma\gamma$ events are required to satisfy the following criteria:

1. There must be at least two identified leptons of the same flavour and at least two photons. The two most energetic leptons and two most energetic photons are used for further analysis. For the excited tau search, it is required that at most one of the two tau jets be an identified electron, and at most one of the two tau jets be an identified muon.
2. In the $e^+e^-\gamma\gamma$ and $\mu^+\mu^-\gamma\gamma$ analyses, the sum of the energies of the two leptons and two photons, $E_{\rm vis}$, must satisfy $E_{\rm vis} > 1.6\ E_{\rm beam}$. In the $\tau^+\tau^-\gamma\gamma$ analysis, the sum of the energies of the two tau jets and two photons must satisfy $0.8\ E_{\rm beam} < E_{\rm vis} < 1.9\ E_{\rm beam}$. The sums of the energies of the two leptons and two photons before cut 2 are plotted in Figure 6.

	After Cut	Data	Total Bkg	ee(γ)	$\mu\mu(\gamma)$	$\tau\tau(\gamma)$	$M_* =$ 80 GeV
ee$\gamma\gamma$	1	33	23.9	18.8	0.0	1.5	69.9
	2	26	17.2	17.0	0.0	0.1	69.6
	3	3	2.3	2.2	0.0	0.0	60.7
	4	2	1.5	1.5	0.0	0.0	58.4
	5	0	1.3	1.3	0.0	0.0	53.0
$\mu\mu\gamma\gamma$	1	5	5.5	0.0	3.4	0.8	75.5
	2	2	2.6	0.0	2.5	0.1	75.2
	3	0	1.4	0.0	1.4	0.0	70.2
	4	0	1.1	0.0	1.1	0.0	67.7
	5	0	0.8	0.0	0.8	0.0	61.3
$\tau\tau\gamma\gamma$	1	33	23.8	1.6	0.1	5.0	54.3
	2	5	4.2	0.3	0.0	3.4	51.4
	3	1	1.2	0.0	0.0	0.9	49.1
	4	0	0.7	0.0	0.0	0.6	45.7
	5	0	0.5	0.0	0.0	0.5	41.8

Table 9: The number of events surviving each cut for background, and selection efficiencies in percent for some example signal Monte Carlos, in the $\ell^+\ell^-\gamma\gamma$ topology. The efficiencies are for the pair production of charged excited leptons which decay photonically. The expected background levels are normalized to the actual integrated luminosity. The statistical error on the background Monte Carlo is small compared to that for data.

3. A significant background after cuts 1 and 2 is from Bhabha scattering or lepton-pair production with final-state radiation. This is reduced by requiring the lepton-photon pair to be isolated. The minimum opening angle among all lepton-photon combinations, $\theta^{\ell\gamma}_{\rm min}$, is required to satisfy $|\cos\theta^{\ell\gamma}_{\rm min}| < 0.90$ for $e^+e^-\gamma\gamma$ and $|\cos\theta^{\ell\gamma}_{\rm min}| < 0.95$ for $\mu^+\mu^-\gamma\gamma$ and $\tau^+\tau^-\gamma\gamma$.

4. The momenta of the two leptons and two photons are now calculated assuming a 4-body final state with no missing energy, using the measured angles of the tracks and clusters. The calculation uses the beam-energy constraint, conserving energy and momentum. It is required that all energies calculated are greater than zero. The momenta of the leptons calculated in this manner are used in cut 5.

5. The final reducible component in the background is from the doubly-radiative-return process $e^+e^- \to Z^0\gamma\gamma \to \ell^+\ell^-\gamma\gamma$. Events with a di-lepton mass, $M_{\ell\ell}$, satisfying 80 GeV $< M_{\ell\ell} <$ 100 GeV are vetoed.

The complete analysis is summarized in Table 9, including an example signal of charged excited leptons with photonic decays. No event survives in any channel, which is consistent with the expectations from Standard Model sources.

The efficiency for observing the pair-production of excited leptons with photonic decays is estimated with Monte Carlo to be about 54% for $e^{*+}e^{*-}$, 62% for $\mu^{*+}\mu^{*-}$ and 42% for $\tau^{*+}\tau^{*-}$, with only a small dependence on the mass of the excited lepton.

4.4.2 $\ell^+\ell^-\gamma$ Final States

Candidate $\ell^+\ell^-\gamma$ events are required to satisfy the following criteria:

1. There must be at least two identified leptons of the same flavour and at least one photon. The two most energetic leptons and the most energetic photon are used for further analysis. For the excited tau search, it is required that at most one of the two tau jets be an identified electron, and at most one of the two tau jets be an identified muon.

2. In the $e^+e^-\gamma$ and $\mu^+\mu^-\gamma$ analyses, the sum of the energies of the two leptons and one photon, $E_{\rm vis}$, must satisfy $E_{\rm vis} > 1.6\ E_{\rm beam}$. In the $\tau^+\tau^-\gamma$ analysis, the sum of the energies of the two tau jets and one photon must satisfy $0.8\ E_{\rm beam} < E_{\rm vis} < 1.9\ E_{\rm beam}$. The sums of the energies of the two leptons and the photon before cut 2 are plotted in Figure 7.

3. A significant background after cuts 1 and 2 is from Bhabha scattering or lepton-pair production with final-state radiation. This is reduced by requiring the lepton-photon pair to be isolated. The minimum opening angle between both lepton-photon combinations, $\theta^{\ell\gamma}_{\rm min}$ is required to satisfy $|\cos\theta^{\ell\gamma}_{\rm min}| < 0.90$ for $e^+e^-\gamma$ and $|\cos\theta^{\ell\gamma}_{\rm min}| < 0.95$ for $\mu^+\mu^-\gamma$ and $\tau^+\tau^-\gamma$. For the e^* search, radiative Bhabha scattering is further suppressed by also requiring that the photon and at least one electron satisfy $|\cos\theta| < 0.7$.

4. The momenta of the two leptons and one photon are now calculated assuming a 3-body final state using the measured angles of the tracks and clusters. The calculation uses the beam-energy constraint, conserving energy and momentum. One initial-state radiation photon along the beam axis is included in the calculation. It is required that all energies calculated are greater than zero. The momenta of the leptons and photon calculated in this manner are used in cut 5, and also to construct the lepton-photon invariant mass for the excited lepton search.

5. The final reducible component in the background is from the radiative-return process $e^+e^- \to Z^0\gamma \to \ell^+\ell^-\gamma$. Events with a di-lepton mass, $M_{\ell\ell}$, satisfying 80 GeV $< M_{\ell\ell} <$ 100 GeV are vetoed.

The complete analysis is summarized in Table 10, including two example mass points for single-production of charged excited leptons with photonic decays. The numbers of events selected in each channel are consistent with the expectations from Standard Model sources.

The lepton-photon mass resolutions are estimated with Monte Carlo to be 0.4–0.5 GeV for excited electrons and muons with photonic decays, and 2–3 GeV for excited taus with photonic decays. The lepton-photon invariant masses, $M_{\ell\gamma}$, are plotted in Figure 8 for the excited muon and tau searches, combining the full 161–172 GeV data. No anomalous structure is apparent. When computing limits for an excited lepton with mass M_*, all events with at least one lepton-photon mass combination satisfying $|M_{\ell\gamma} - M_*| < \Delta$ are considered signal candidates, where $\Delta = 2$ and 5 GeV for the excited muon and tau search, respectively. The efficiency for observing the single-production of excited leptons with photonic decays is estimated with Monte Carlo to be about 70% for $\mu^*\mu$ and 40% for $\tau^*\tau$, including the mass window constraint, with some dependence on the mass of the excited lepton. The excited electron results are summarized after the analysis described in Section 4.4.3.

4.4.3 e* Single Production: eγ Topology

A significant fraction of singly-produced e* events would have the recoil electron at a small polar angle, outside the detector acceptance, making the search for the eγ final state also interesting.

After removing events which pass the eeγ selection described in Section 4.4.2, candidate eγ events are required to satisfy the following criteria:

1. There must be at least one identified electron and one identified photon. The most energetic electron and photon are used for further analysis.
2. The energy sum of the electron and photon, $E_{\rm vis}$, must satisfy $E_{\rm vis} > 0.8\ E_{\rm beam}$.
3. A significant background after cuts 1 and 2 is from Bhabha scattering with final-state radiation. This is reduced by requiring the electron-photon pair to be isolated. The opening angle between the electron and photon, $\theta^{\ell\gamma}_{\rm min}$, is required to satisfy $|\cos\theta^{\ell\gamma}_{\rm min}| < 0.95$.
4. Bhabha scattering is further suppressed by requiring the photon to satisfy $|\cos\theta_\gamma| < 0.7$, and that the event thrust axis formed with the observed lepton and photon satisfy $|\cos\theta_{\rm thrust}| < 0.9$.
5. The momenta of the electron and photon are now calculated assuming a 2-body final state plus one electron missing along the beam axis using only the measured polar angles of the observed electron and photon. The calculation uses the beam-energy constraint, conserving energy and momentum. It is required that all energies calculated are greater than zero. The momenta of the electron and photon calculated in this manner are used to construct the electron-photon invariant mass for the excited electron search.

The analysis is summarized in Table 10, including two example mass points for single-production of charged excited electrons with photonic decays. The number of events selected is consistent with the expectation from Standard Model sources.

Events which survive in either the $e^+e^-\gamma$ or eγ analysis are considered as excited electron candidates. The electron-photon mass resolutions are estimated with Monte Carlo to be 0.4–0.5 GeV in both channels. The electron-photon invariant masses are plotted in Figure 9, combining the full 161–172 GeV data. No anomalous structure is apparent. When computing limits for an excited electron with mass M_*, events satisfying $|M_{e\gamma} - M_*| < 2$ GeV are considered signal candidates. The efficiency for observing the single-production of excited electrons with photonic decays is estimated with Monte Carlo to be 35–70%, including the mass window constraint, depending on the mass of the excited electron.

5 Results

The numbers of expected signal events are evaluated from the total production cross-sections, the total integrated luminosity, and the estimated detection efficiencies for the various analyses.

	After Cut	Data	Total Bkg	ee(γ)	$\mu\mu(\gamma)$	$\tau\tau(\gamma)$	$M_* =$ 80 GeV	$M_* =$ 140 GeV
eeγ	1	320	310.9	219.4	0.0	4.0	7.5	11.0
	2	171	198.3	197.6	0.0	0.1	7.0	10.9
	3	10	12.4	12.3	0.0	0.0	3.4	7.1
	4	10	12.4	12.3	0.0	0.0	3.4	7.0
	5	6	10.9	10.9	0.0	0.0	2.8	5.9
eγ	1	3046	2384.5	1135.4	0.0	15.9	74.4	84.6
	2	669	722.1	714.3	0.0	4.2	73.3	84.5
	3	620	669.0	662.2	0.0	3.6	73.2	84.0
	4	61	81.1	78.7	0.0	1.8	42.2	62.9
	5	52	73.0	70.8	0.0	1.6	42.2	62.4
$\mu\mu\gamma$	1	76	55.9	0.0	23.3	2.5	85.0	84.6
	2	16	15.6	0.0	15.5	0.1	78.6	83.9
	3	11	12.5	0.0	12.3	0.0	77.7	81.5
	4	11	12.3	0.0	12.2	0.0	77.6	81.2
	5	9	8.1	0.0	8.1	0.0	70.5	67.7
$\tau\tau\gamma$	1	193	156.1	34.9	0.4	20.0	62.7	56.8
	2	23	23.4	8.1	0.3	13.2	57.1	54.1
	3	13	14.1	3.9	0.2	8.7	56.0	52.5
	4	13	12.6	3.4	0.2	7.9	54.9	51.4
	5	8	9.7	3.2	0.1	5.4	50.5	43.2

Table 10: The number of events surviving each cut for background, and the selection efficiencies in percent for excited lepton signal Monte Carlo, in the single-production search. The signal Monte Carlo corresponds to the coupling assignment $f = f'$, but with 100% photonic decays. The expected background levels are normalized to the actual integrated luminosity. The efficiencies for the $e^+e^-\gamma$ and eγ excited electron single-production topologies are exclusive, and can be summed for the total selection efficiency. The statistical error on the background Monte Carlo is small compared to that for data.

Mode		Mass Limit (GeV)
$N \to eW$	Dirac	79.1
	Majorana	69.8
$N \to \mu W$	Dirac	78.5
	Majorana	68.7
$N \to \tau W$	Dirac	69.0
	Majorana	54.4
$L^- \to \nu_\ell W^-$		80.2
$L^- \to NW^-$		81.5 (with $\Delta M > 8.4$)

Table 11: 95% confidence level lower mass limits on unstable neutral heavy leptons obtained from the combined data collected at $\sqrt{s} = 161$, 170 and 172 GeV.

In the pair-production searches, the production cross-section is relatively model-independent, and limits on the masses of the heavy or excited lepton can be obtained directly. In the single-production searches, the production cross-section depends on parameters within the model, so limits on those parameters, as a function of the new particle masses, are inferred instead. The systematic errors on the total number of expected signal events are estimated from: the statistical error on the Monte Carlo estimate of the detection efficiency, 1–2%; the error due to the interpolation used to infer the efficiency at arbitrary masses from the limited number of Monte Carlo samples, 2–5%; the error on the integrated luminosity, 0.6%; the uncertainties in modelling the lepton identification cuts are estimated by comparing the efficiency for selecting leptons in events from Standard Model processes between data and Monte Carlo, and are found to be in the range 2–5%; the uncertainty in the modelling of the photon conversion finder used in the $\ell^+\ell^-\gamma(\gamma)$ analyses is estimated by comparing the ratio of non-converting to converting photons in data and Standard Model process Monte Carlo, and is found to be 1% per photon in the event. The errors are considered to be independent and are added in quadrature to give the total systematic error, which is always less than 10%. The systematic error is incorporated into the limits inferred from the data using the method described in Reference [41]. The final limits are computed considering the background levels expected in the analysis [42], including the full 161–172 GeV dataset.

For the flavour-mixing heavy lepton decays in which the pair-produced heavy leptons undergo CC decays into light leptons, 95% confidence level lower limits on the mass of the heavy lepton are shown in Table 11. These results are valid for a mixing angle squared, ζ^2, greater than about 10^{-12}. In the case that a heavy charged lepton, $L^\pm$, decays into a stable heavy neutral lepton, N, the exclusion region depends on both M_L and M_N. The excluded region is shown in Figure 10. From that figure, if the charged heavy lepton is at least 8.4 GeV more massive than the neutral heavy lepton, its mass is less than 81.5 GeV at the 95% confidence level.

The mass limits on excited leptons are somewhat better than for the heavy lepton case, primarily due to the vector couplings leading to larger production cross-sections. The mass limits inferred from the pair-production searches are shown in Table 12. Since the branching ratio to either photons or W-bosons is essentially 100% in the mass range that our pair-production searches are sensitive to, only the dominant decay is used when computing the mass limits.

Flavour	Coupling	Dominant Decay	Mass Limit (GeV)
e^*	$f = f'$	Photonic	85.0
μ^*	$f = f'$	Photonic	85.3
τ^*	$f = f'$	Photonic	84.6
e^*	$f = -f'$	Charged	81.3
μ^*	$f = -f'$	Charged	81.3
τ^*	$f = -f'$	Charged	81.3
ν_e^*	$f = f'$	Charged	84.1
ν_μ^*	$f = f'$	Charged	83.9
ν_τ^*	$f = f'$	Charged	79.4
ν_e^*	$f = -f'$	Photonic	84.9
ν_μ^*	$f = -f'$	Photonic	84.9
ν_τ^*	$f = -f'$	Photonic	84.9

Table 12: 95% confidence level lower mass limits for the different excited leptons obtained from the pair-production searches. The coupling assumption affects the branching ratio.

From the single-production searches, limits on the ratio of the coupling to the compositeness scale, f/Λ, are shown in Figure 11 for two example coupling assumptions. Since the branching ratio of the excited lepton decays via the different vector bosons is arbitrary, example coupling assignments $f = \pm f'$ are used to calculate these branching ratios and then the photonic and CC decay results are combined for the limits.

6 Conclusion

We have analysed a data sample corresponding to an integrated luminosity of 10.3 pb^{-1} at 170.3 and 172.3 GeV, collected with the OPAL detector at LEP, to search for the production of unstable heavy and excited leptons. No evidence for their existence was found, and limits on masses and couplings were established. From the search for the pair production of heavy and excited leptons, lower mass limits were established. From the search for the single production of excited leptons, upper limits on the ratio of the coupling to the compositeness scale were derived. These limits substantially improve those from previous LEP searches.

7 Acknowledgements

We particularly wish to thank the SL Division for the efficient operation of the LEP accelerator at all energies and for their continuing close cooperation with our experimental group. We thank our colleagues from CEA, DAPNIA/SPP, CE-Saclay for their efforts over the years on the time-of-flight and trigger systems which we continue to use. In addition to the support staff at our own institutions we are pleased to acknowledge the
Department of Energy, USA,

National Science Foundation, USA,
Particle Physics and Astronomy Research Council, UK,
Natural Sciences and Engineering Research Council, Canada,
Israel Science Foundation, administered by the Israel Academy of Science and Humanities,
Minerva Gesellschaft,
Benoziyo Center for High Energy Physics,
Japanese Ministry of Education, Science and Culture (the Monbusho) and a grant under the Monbusho International Science Research Program,
German Israeli Bi-national Science Foundation (GIF),
Bundesministerium für Bildung, Wissenschaft, Forschung und Technologie, Germany,
National Research Council of Canada,
Hungarian Foundation for Scientific Research, OTKA T-016660, T023793 and OTKA F-023259.

References

[1] "Review of Particle Physics" R.M. Barnett *et al.*, Phys. Rev. D54 (1996).

[2] A. Djouadi, D. Schaile, C. Verzegnassi, *et al.*, Report of the Working Group "Extended Gauge Models" in Proceedings of the Workshop "e^+e^- Collisions at 500 GeV: The Physics Potential", P. Zerwas, (ed.) Report DESY 92-123A+B.

[3] ALEPH Collaboration, D. Decamp *et al.*, Phys. Lett. B236 (1990) 511;
OPAL Collaboration, M.Z. Akrawy *et al.*, Phys. Lett. B240 (1990) 250;
OPAL Collaboration, M.Z. Akrawy *et al.*, Phys. Lett. B247 (1990) 448;
L3 Collaboration, B. Adeva *et al.*, Phys. Lett. B251 (1990) 321;
DELPHI Collaboration, P. Abreu *et al.*, Phys. Lett. B274 (1992) 230.

[4] OPAL Collaboration, G. Alexander *et al.*, Phys. Lett. B385 (1996) 433.

[5] L3 Collaboration, M. Acciarri *et al.*, Phys. Lett. B377 (1996) 304;
ALEPH Collaboration, D. Buskulic *et al.*, Phys. Lett. B384 (1996) 439.

[6] OPAL Collaboration, K. Ackerstaff *et al.*, Phys. Lett. B393 (1997) 217.

[7] L3 Collaboration, M. Acciarri *et al.*, "Search for Heavy Neutral and Charged Leptons in e^+e^- Annihilation at $\sqrt{s}$ = 161 and 172 GeV", CERN-PPE/97-75, submitted to Phys. Lett. B.

[8] OPAL Collaboration, M.Z. Akrawy *et al.*, Phys. Lett. B257 (1990) 531;
ALEPH Collaboration, D. Decamp *et al.*, Phys. Lett. B250 (1990) 172;
DELPHI Collaboration, P. Abreu *et al.*, Z. Phys. C53 (1992) 41;
L3 Collaboration, M. Acciarri *et al.*, Phys. Lett. B353 (1995) 136.

[9] OPAL Collaboration, G. Alexander *et al.*, Phys. Lett. B386 (1996) 463.

[10] L3 Collaboration, M. Acciarri *et al.*, Phys. Lett. B370 (1996) 211;
DELPHI Collaboration, P. Abreu *et al.*, Phys. Lett. B380 (1996) 480;
ALEPH Collaboration, D. Buskulic *et al.*,Phys. Lett. B385 (1996) 445.

[11] OPAL Collaboration, K. Ackerstaff *et al.*, Phys. Lett. B391 (1997) 197.

[12] DELPHI Collaboration, P. Abreu *et al.*, Phys. Lett. B393 (1997) 245;
L3 Collaboration, M. Acciarri *et al.*, Phys. Lett. B401 (1997) 139.

[13] H1 Collaboration, I. Abt *et al.*, Nucl. Phys. B396 (1993) 3;
ZEUS Collaboration, M. Derrick *et al.*, Z. Phys. C65 (1994) 627.

[14] OPAL Collaboration, G. Alexander *et al.*, Phys. Lett. B377 (1996) 222.

[15] OPAL Collaboration, K. Ackerstaff *et al.*, Phys. Lett. B391 (1997) 221;
OPAL Collaboration, K. Ackerstaff *et al.*, "Tests of the Standard Model and Constraints on New Physics from Measurements of Fermion-pair Production at 130-172 GeV at LEP", CERN-PPE/97-101, submitted to Z. Phys C.

[16] A. Djouadi, Z. Phys. C63 (1994) 317, and references therein.

[17] E. Nardi, E. Roulet and D. Tommasini, Phys. Lett. B344 (1995) 225.

[18] F. Boudjema, A. Djouadi and J.L. Kneur, Z. Phys. C57 (1993) 425.

[19] OPAL Collaboration, K. Ahmet *et al.*, Nucl. Instr. Meth. A305 (1991) 275;
P.P. Allport *et al.*, Nucl. Instr. Meth. A324 (1993) 34;
P.P. Allport *et al.*, Nucl. Instr. Meth. A346 (1994) 476;
B.E. Anderson *et al.*, IEEE Trans. Nucl. Sci. 41 (1994) 845.

[20] J.H. Kühn, A. Reiter and P.M. Zerwas, Nucl. Phys. B272 (1986) 560.

[21] T. Sjöstrand, Comp. Phys. Comm. 82 (1994) 74.

[22] S. Jadach, W. Placzek and B.F.L. Ward, Phys. Lett. B390 (1997) 298.

[23] D. Karlen, Nucl. Phys. B289 (1987) 23.

[24] S. Jadach, B.F.L. Ward and Z. Wąs, Comp. Phys. Comm. 79 (1994) 503.

[25] G. Marchesini *et al.*, Comp. Phys. Comm. 67 (1992) 465.

[26] A. Buijs *el al.*, Phys. Rev. D54 (1996) 4244.

[27] R. Bhattacharya, J. Smith and G. Grammer, Phys. Rev. D15 (1977) 3267;
J. Smith, J.A.M. Vermaseren and G. Grammer, Phys. Rev. D15 (1977) 3280.

[28] J. Hilgart, R.Kleiss and F. Le Diberder, Comp. Phys. Comm. 75 (1993) 191.

[29] F.A. Berends, R. Pittau and R. Kleiss, Comp. Phys. Comm. 85 (1995) 437.

[30] J. Fujimoto *et al.*, Comp. Phys. Comm. 100 (1996) 128.

[31] F.A. Berends and R. Kleiss, Nucl. Phys. B186 (1981) 22.

[32] G. Montagna *et al.*, Nucl. Phys. B452 (1995) 161.

[33] J. Allison *et al.*, Nucl. Instr. Meth. A317 (1992) 47.

[34] OPAL Collaboration, M.Z. Akrawy *el al.*, Phys. Lett. B253 (1990) 511.

[35] N. Brown and W.J. Stirling, Phys. Lett. B252 (1990) 657;
S. Bethke, Z. Kunszt, D. Soper and W.J. Stirling, Nucl. Phys. B370 (1992) 310;
S. Catani *et al.*, Nucl. Phys. B269 (1991) 432;
N. Brown and W. J. Stirling, Z. Phys. C53 (1992) 629.

[36] OPAL Collaboration, R. Akers *et al.*, Phys. Lett. B327 (1994) 411.

[37] OPAL Collaboration, K. Ackerstaff *et al.*, "Search for Anomalous Production of Photonic Events with Missing Energy in e^+e^- Collisions at $\sqrt{s}$ = 130-172 GeV", to be submitted to Z. Phys. C.

[38] OPAL Collaboration, G. Alexander *et al.*, Z. Phys. C52 (1991) 175.

[39] M. Hauschild *et al.*, Nucl. Instr. and Meth. A314 (1992) 74.

[40] OPAL Collaboration, P. Acton *et al.*, Z. Phys. C58 (1993) 523.

[41] R.D. Cousins and V.L. Highland, Nucl. Instr. Meth. A 320 (1992) 331.

[42] Formulae 28.40 in Reference [1].

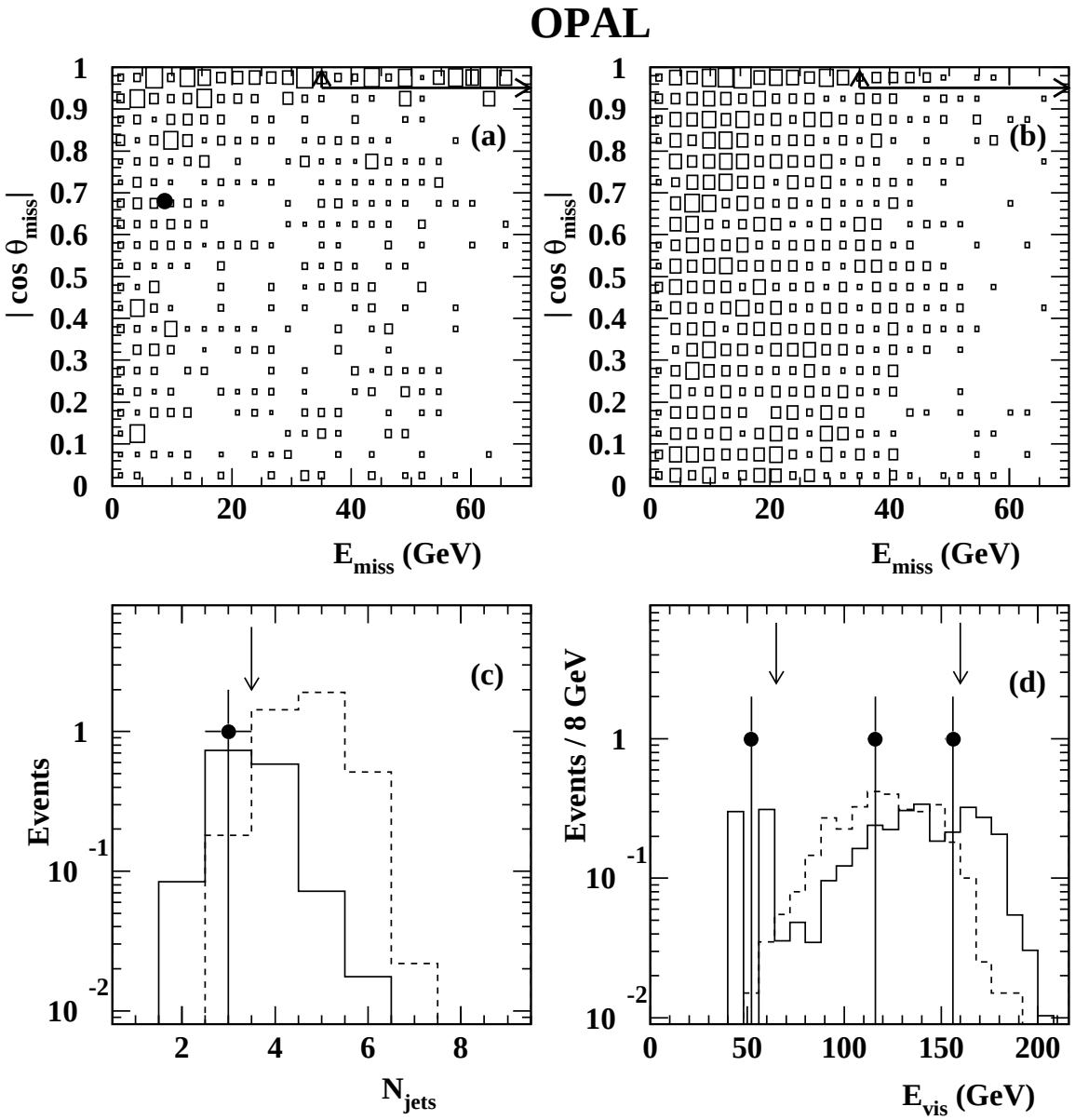

Figure 1: The distributions of $|\cos\theta_{\rm miss}|$ versus $E_{\rm miss}$ are shown in (a) for the background processes (box) and the selected $\mathrm{N} \to \mathrm{eW}$ event among the data (filled circle) after cut 2; the distribution for the $\mathrm{N\bar{N}}$ signal is shown in (b) for a Dirac N (with $M_{\rm N} = 75$ GeV). The distributions for the number of reconstructed jets for the case $\mathrm{N} \to \mathrm{eW}$ after cut 3 are shown in (c) for the data (filled circles), the background processes (solid line), and the $\mathrm{N\bar{N}}$ signal (Dirac N, with $M_{\rm N} = 75$ GeV) (broken line). For the case $\mathrm{N} \to \tau\mathrm{W}$ the visible energy ($E_{\rm vis}$) distributions after cut 4 are shown in (d) for the data (filled circles), the background processes (solid line), and the $\mathrm{N\bar{N}}$ signal (broken line) for a Dirac N with $M_{\rm N} = 65$ GeV. The arrows correspond to the cut values. The corresponding distributions for a Majorana N are similar.

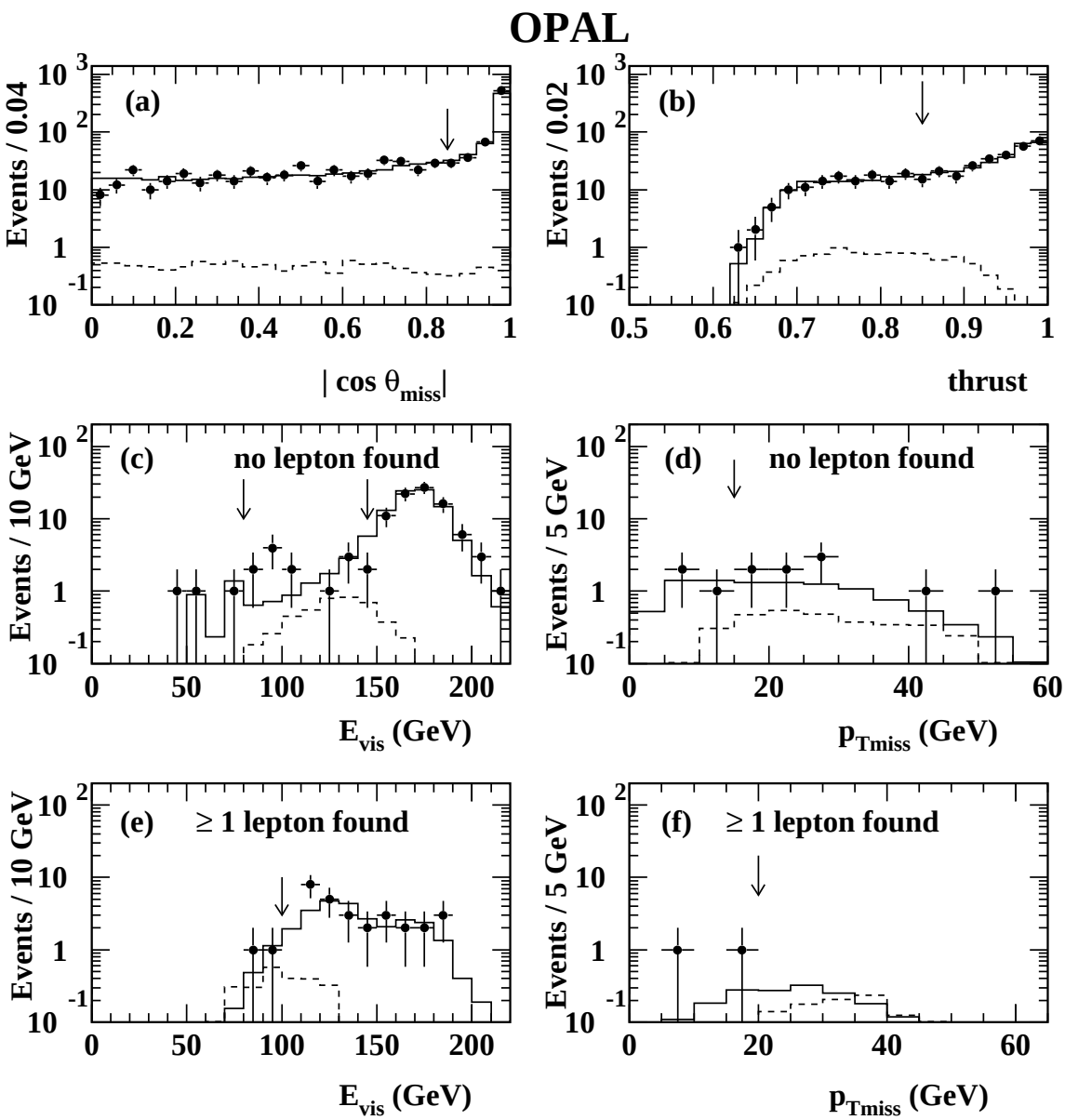

Figure 2: The $|\cos\theta_{\rm miss}|$ distribution after cut 2 (a) and the thrust distribution after cut 3 (b), for the $\rm L^+L^-$ candidate selection with $\rm L^- \to \nu_\ell W^-$. In the case where no isolated lepton is found, the distributions after cut 4 for the visible energy and the missing transverse momentum are shown respectively in (c) and (d). In the case where at least one isolated lepton is found, the corresponding distributions are shown respectively in (e) and (f). The filled circles are the data, the solid lines are the background processes, and the broken lines are the $\rm L^+L^-$ signal with $\rm L^- \to \nu_\ell W^-$ for the case where $M_{\rm L} = 80$ GeV. The arrows correspond to the cut values.

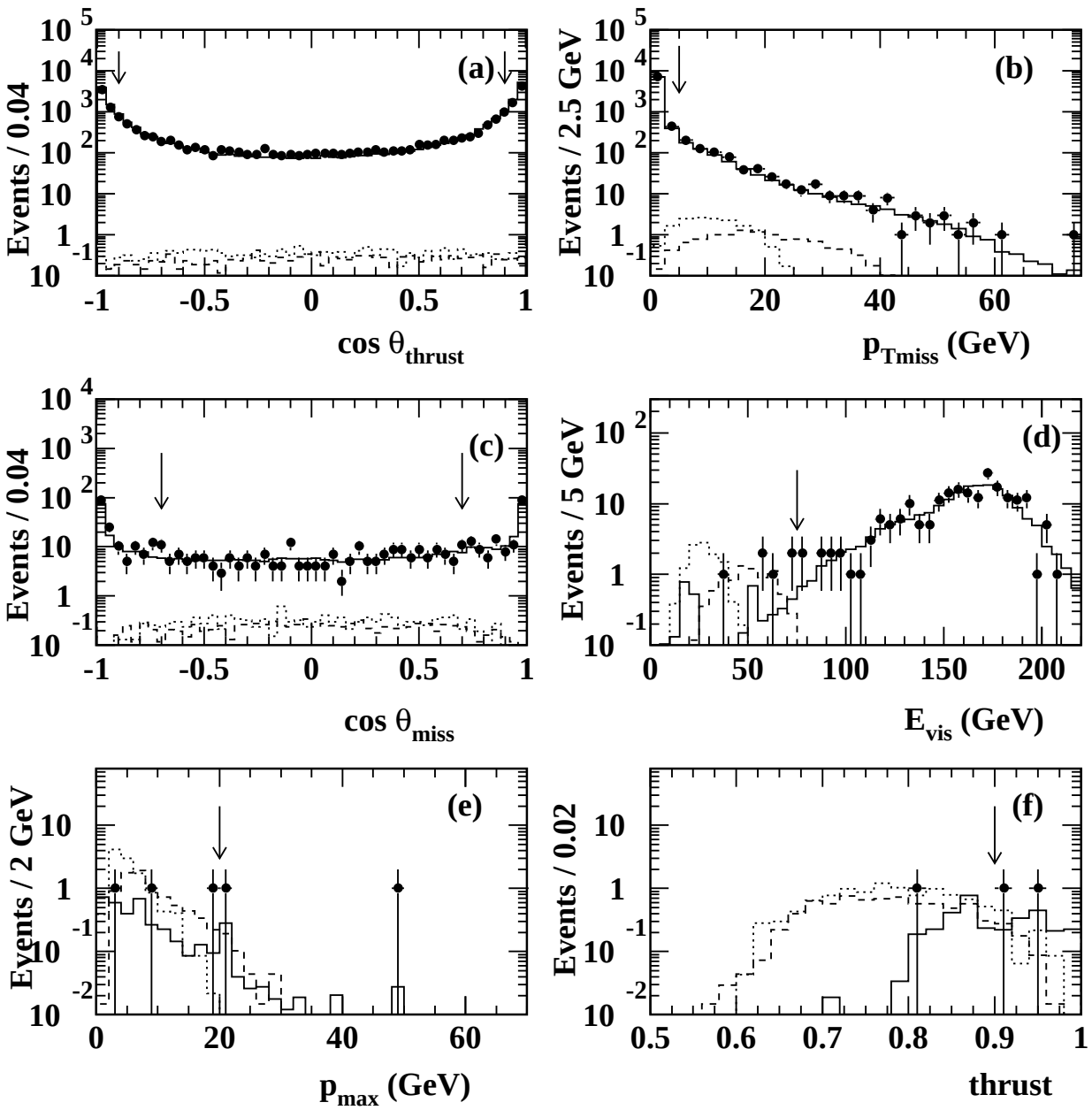

Figure 3: The plots show the distributions for the L^+L^- candidate selection for the case $L^- \to NW^-$ for the data (filled circles), the background processes (solid lines), and the L^+L^- signal with $L^- \to NW^-$ for the cases ($M_L = 75, M_N = 60$) GeV (dotted lines) and ($M_L = 80, M_N = 50$) GeV (broken lines $\times 5$) respectively for $\cos\theta_{\rm thrust}$ after cut 2 (a), $p_{\rm Tmiss}$ after cut 3 (b), $\cos\theta_{\rm miss}$ after cut 4 (c), $E_{\rm vis}$ after cut 5 (d), $p_{\rm max}$ after cut 6 (e), and the thrust value after cut 7 (f). The arrows correspond to the cut values.

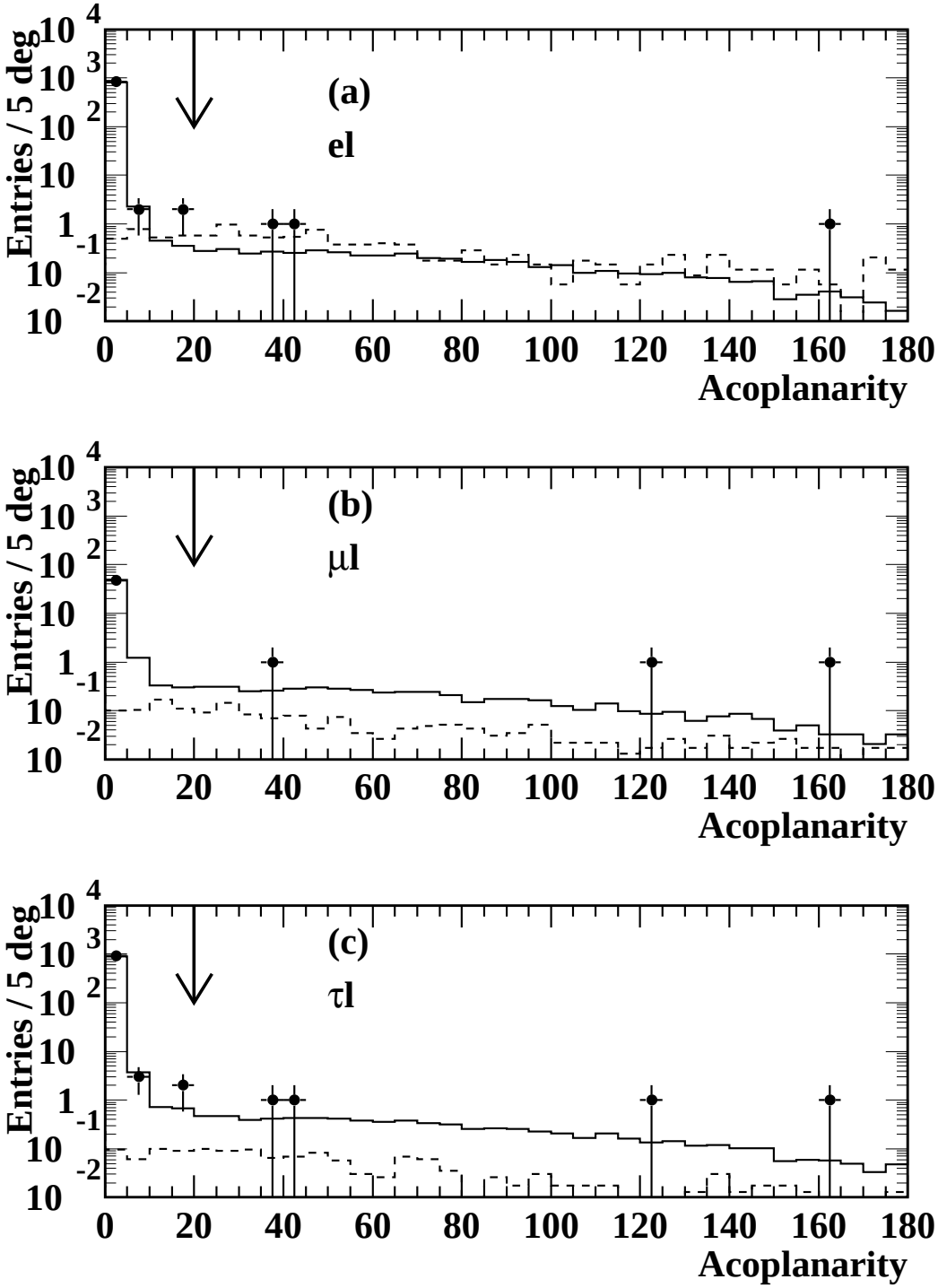

Figure 4: ℓ^* single production, charged decays: the acoplanarity angle between the two observed leptons, before the cut on acoplanarity angle. (a) is for e^* and ν_e^*, (b) is for μ^* and ν_μ^* and (c) is for τ^* and ν_τ^*. The solid line is the sum of all Standard Model background Monte Carlo, the dashed lines are $\ell^{*\pm}\ell^{\mp}$ (charged decay) Monte Carlo with a mass of 80 GeV normalized to $f/\Lambda = (200\ \text{GeV})^{-1}$, and the filled circles are the data. The arrows show the cut value of 20°.

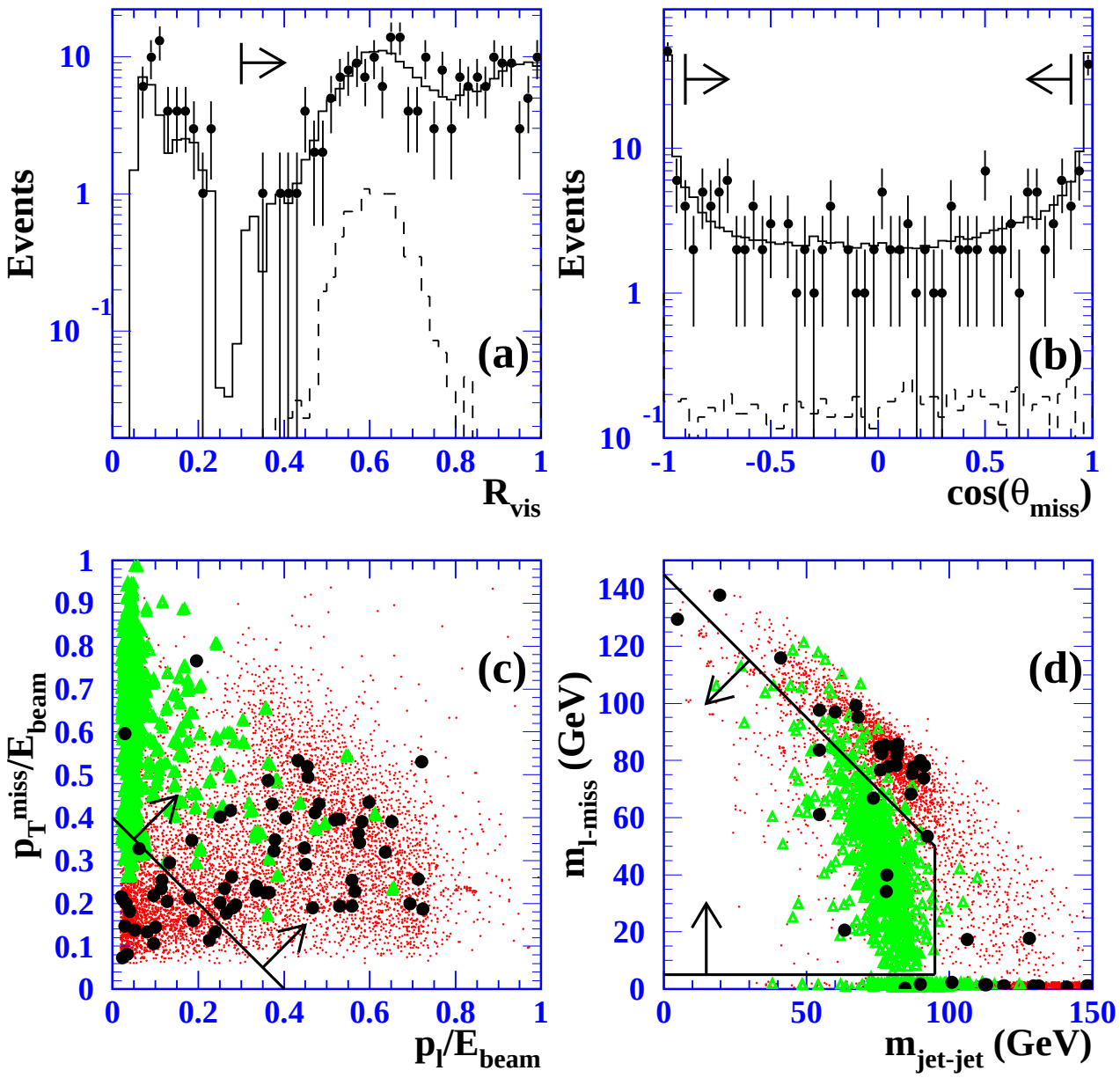

Figure 5: Single-production of charged excited leptons with CC decays, with the cuts applied sequentially. (a) is the event visible energy scaled to $\sqrt{s}$, and (b) is cosine of the polar angle of the missing momentum. In (a) and (b), the filled circles are the data, the solid line is the sum of all Standard Model background Monte Carlo, and the dashed line is excited electron single-production Monte Carlo with $M_* = 170$ GeV and arbitrary normalisation. (c) is the component of the missing momentum transverse to the beam axis *vs.* the lepton momentum, and (d) is the invariant mass of the lepton-neutrino *vs.* the invariant mass of the jet-jet pair. In (c) and (d), the filled circles are the data, the dots are the Standard Model background Monte Carlo, and the triangles are excited electron single production Monte Carlo with $M_* = 170$ GeV. The arrows indicate the region accepted by the cuts on these quantities.

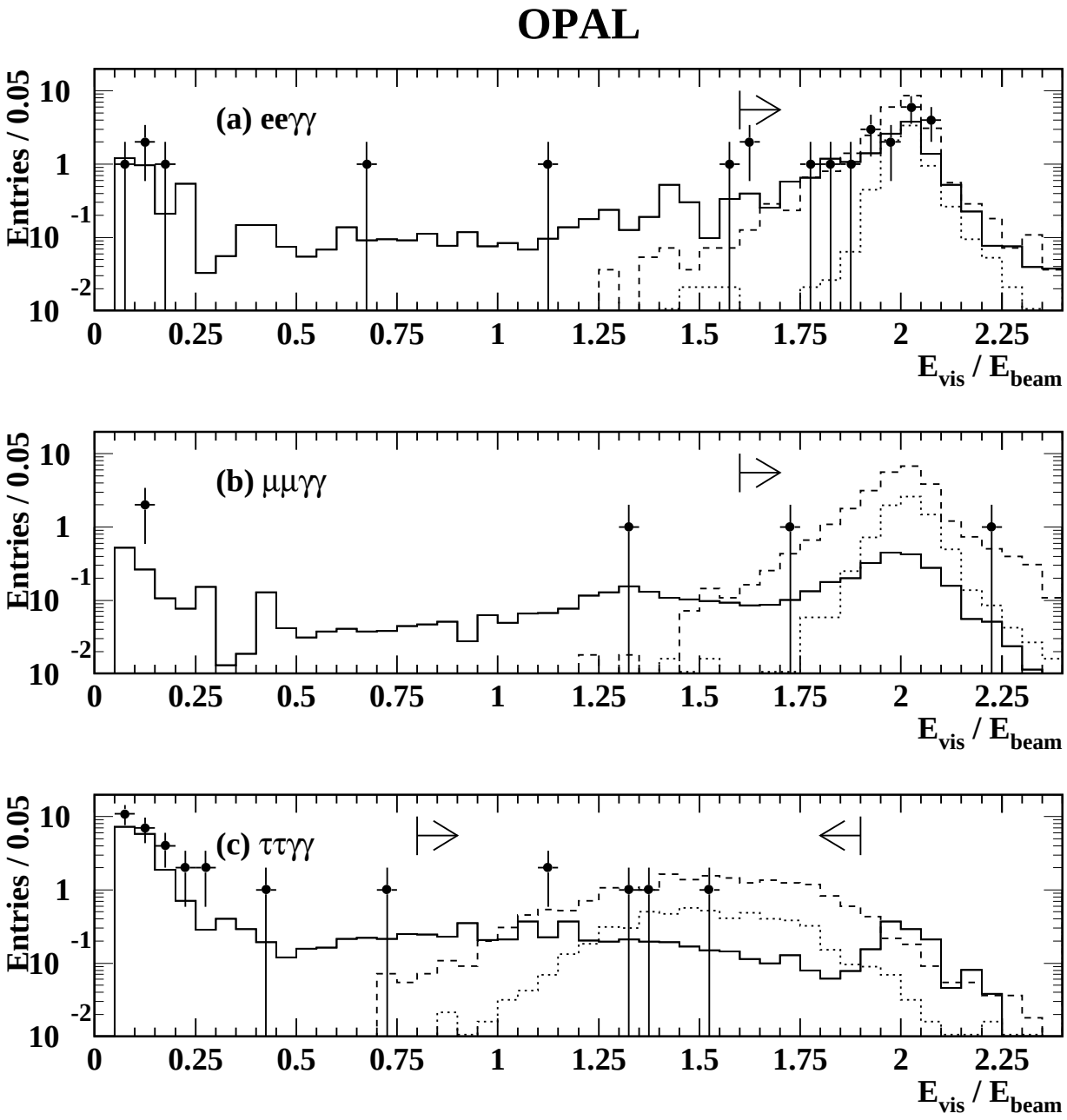

Figure 6: The sums of the energies of the two most energetic leptons and two most energetic photons, after requiring at least two leptons of the same flavour and two photons in the event. (a) is for $e^+e^-\gamma\gamma$, (b) is for $\mu^+\mu^-\gamma\gamma$ and (c) is for $\tau^+\tau^-\gamma\gamma$. The dashed and dotted lines are $\ell^{*+}\ell^{*-}$ photonic-decay signal Monte Carlo with masses of 70 and 85 GeV, respectively, the solid lines are the sum of all of the Standard Model background Monte Carlo and the filled circles are the data. The arrows indicate the cut positions.

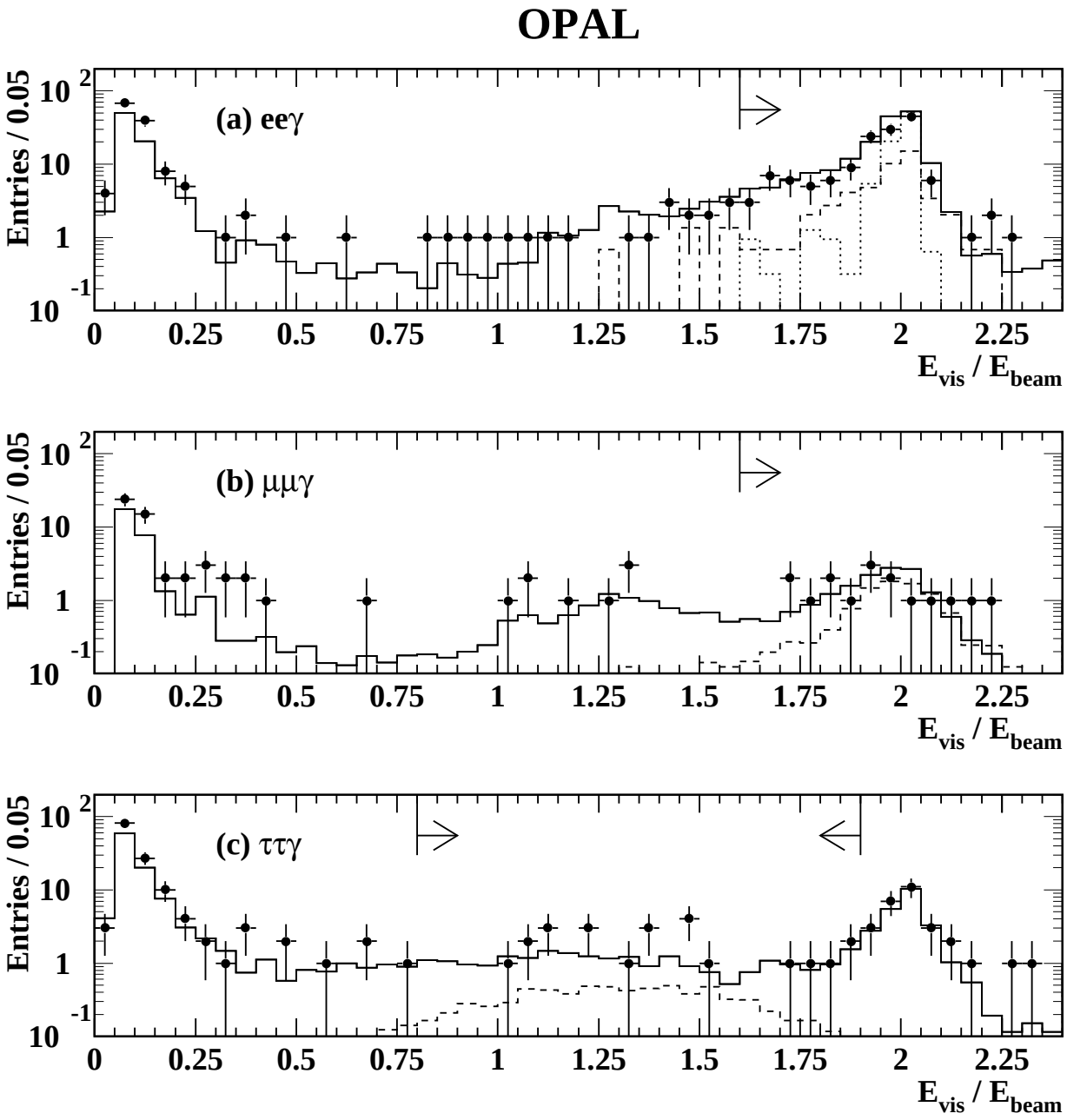

Figure 7: The sums of the energies of the two most energetic leptons and most energetic photon, after requiring at least two leptons of the same flavour and one photon in the event. (a) is for $e^+e^-\gamma$, (b) is for $\mu^+\mu^-\gamma$ and (c) is for $\tau^+\tau^-\gamma$. The dashed and dotted lines are signal Monte Carlo with f/Λ =(200 GeV)$^{-1}$ and with an $\ell^{*\pm}$ mass of 140 GeV and 170 GeV, respectively, the solid lines are the sum of all of the Standard Model background Monte Carlo and the filled circles are the data. The arrows indicate the cut positions.

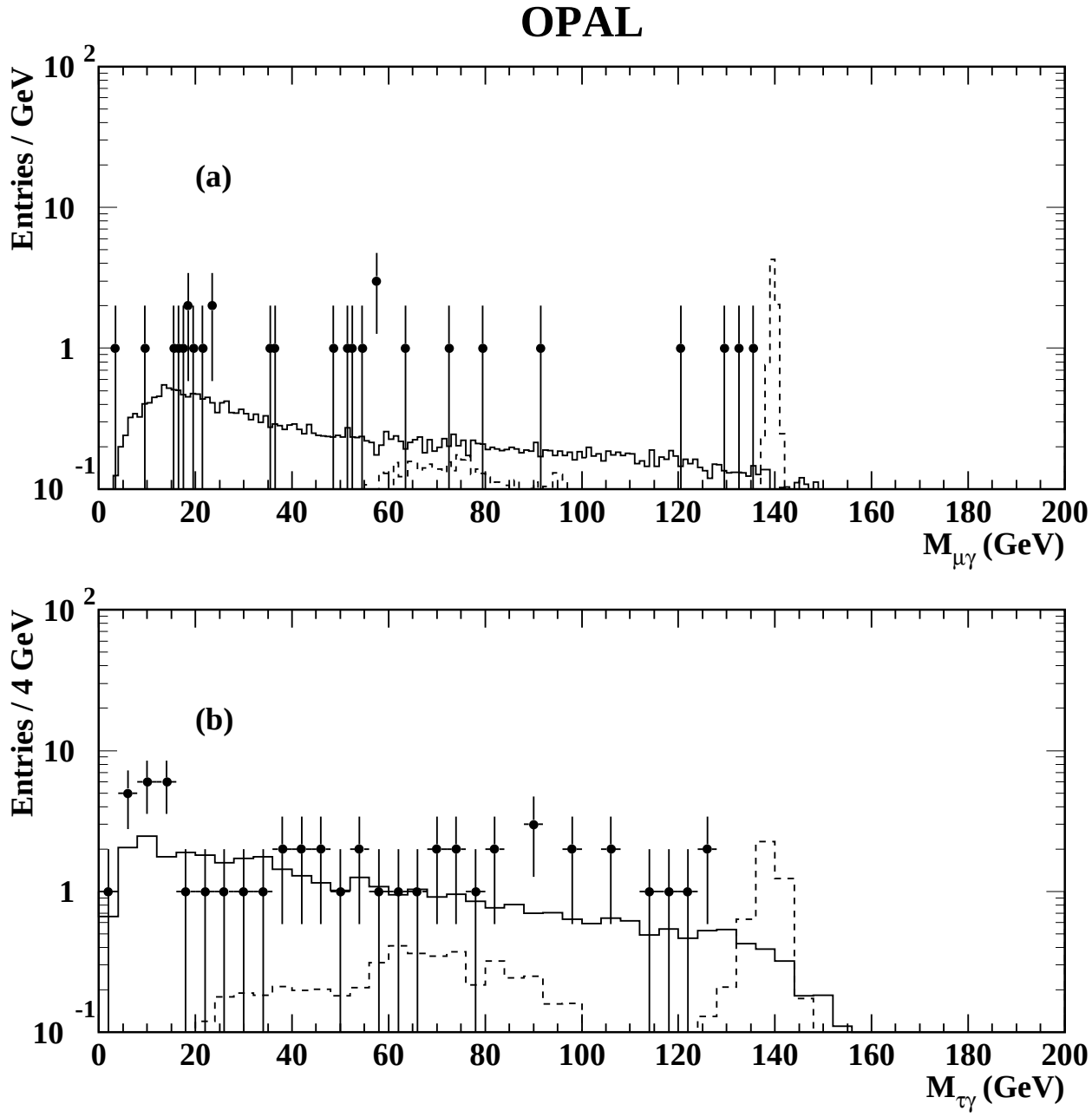

Figure 8: Single production of charged excited leptons with photonic decays: $\ell^{\pm}\gamma$ invariant mass distributions after all cuts for the full 161–172 GeV data set. (a) is $\mu^+\mu^-\gamma$ and (b) is $\tau^+\tau^-\gamma$. The dashed lines are signal Monte Carlo with f/Λ =(100 GeV)$^{-1}$ and with an $\ell^{*\pm}$ mass of 140 GeV, the solid lines are the sum of all of the Standard Model background Monte Carlo and the filled circles are the data. There are two entries per event.

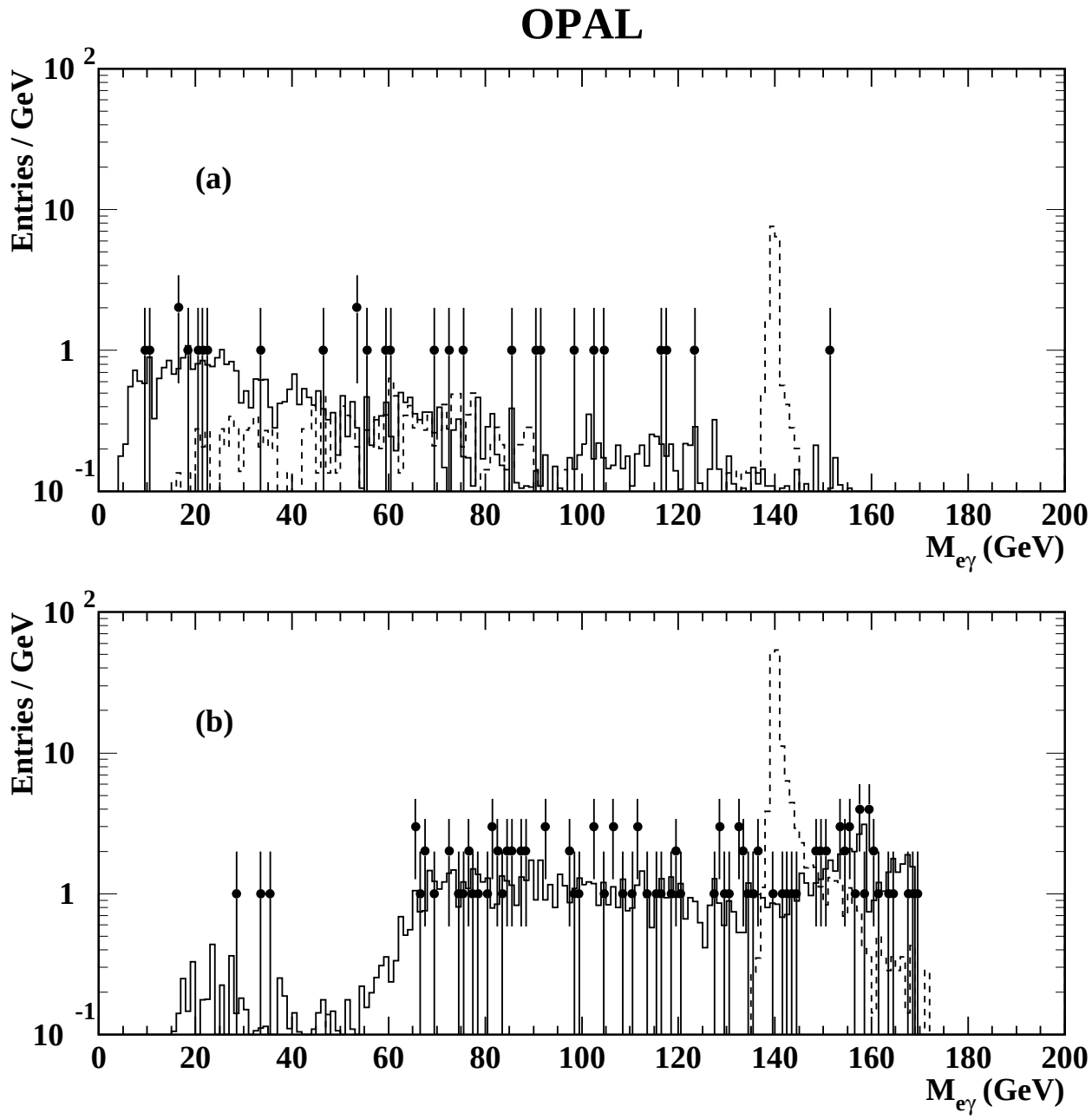

Figure 9: Single production of charged excited electrons with photonic decays: $e\gamma$ invariant mass distributions after all cuts for the full 161–172 GeV data set. (a) The $e^+e^-\gamma$ analysis and (b) the $e\gamma$ (missing electron) topology. The dashed lines are signal Monte Carlo with $f/\Lambda = (500\ \mathrm{GeV})^{-1}$ and with an $e^{*\pm}$ mass of 140 GeV, the solid lines are the sum of all of the Standard Model background Monte Carlo and the filled circles are the data. (a) has two entries per event.

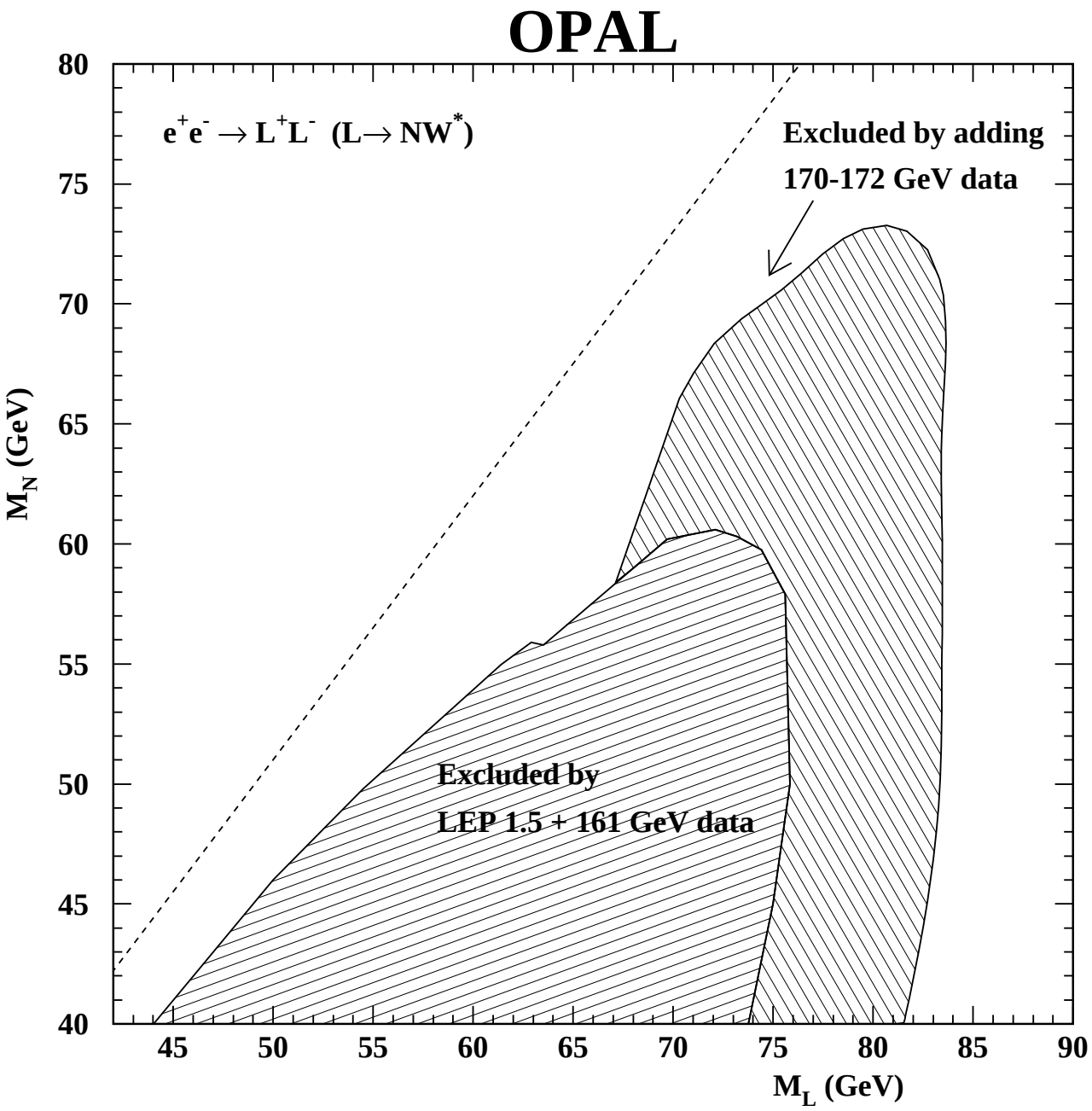

Figure 10: Excluded region in the $(M_{\rm L}, M_{\rm N})$ plane for $\rm L^+L^-$ production in the case where $\rm L^- \to NW^-$. The two hatched regions indicated the previous (LEP 1.5 at $\sqrt{s}$ = 130 and 136 GeV, and the $\sqrt{s} = 161$ GeV data) and new (170-172 GeV data) analyses.

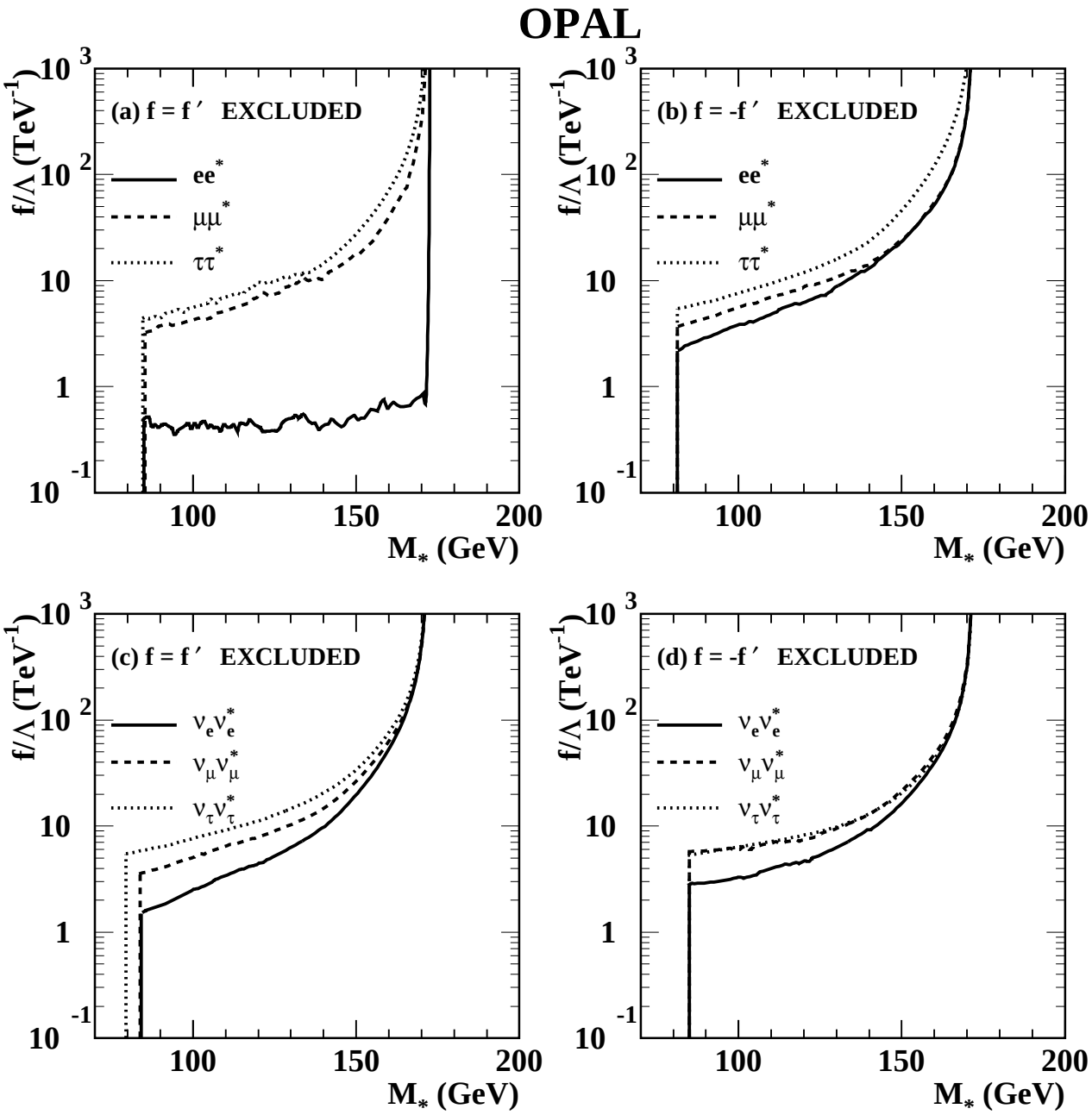

Figure 11: 95% confidence level upper limits on the ratio of the coupling to the compositeness scale, f/Λ, as a function of the excited lepton mass. (a) shows the limits on e*, μ^* and τ^* with $f = f'$, (b) shows the limits on e*, μ^* and τ^* with $f = -f'$, (c) shows the limits on $\nu_{\rm e}^*$, ν_μ^* and ν_τ^* with $f = f'$, and (d) shows the limits on $\nu_{\rm e}^*$, ν_μ^* and ν_τ^* with $f = -f'$. The regions above and to the left of the curves are excluded by the single- and pair-production searches, respectively.